Research Report, June 1995
Project No. 9 on
NASA Cooperative Agreement
* NCC 2-374

APPENDIX A

UNIVERSITY OF CALIFORNIA

Los Angeles

Design and Testing of an Automated System Using Thermochromatic Liquid Crystals to Determine Local Heat Transfer Coefficients for an Impinging Jet

A thesis submitted in partial satisfaction of the
requirements for the degree of Master of Science
in Mechanical Engineering

by

Benjamin Tan

1995

The thesis of Benjamin Tan is approved.

Chang-Jin Kim

Adrienne G. Lavine

Anthony F. Mills, Committee Chair

University of California, Los Angeles

1995

Dedication

To my parents

Table of Contents

List of Symbols

c_p	specific heat at constant pressure	[J/kg K]
D	nozzle inner diameter	[m]
erfc	complementary error function	[]
exp	exponential function	[]
h_c	convective heat transfer coefficient	[W/m^2 K]
k	thermal conductivity	[W/m K]
$\dot{m}$	mass flow rate of air	[kg/s]
Nu	Nusselt number evaluated at TLC transition temperature, h_cD/k	[]
Pr	Prandtl number	[]
r	recovery factor	[]
Re	Reynolds number based on nozzle diameter, $4\dot{m}/\pi\mu D$	[]
t	transition time of TLC	[s]
T	temperature	[K]
z	distance from the stagnation point	[m]

Greek Symbols

α	thermal diffusivity	[m^2/s]
θ	temperature excess, $\theta=T-T_0$	[K]
ϕ	non-dimensional temperature, $\phi = \left(T(x,t) - T_o\right)/\left(T_e(t) - T_o\right)$	[]
ρ	density	[kg/m^3]
τ	dummy variable for t used in integration	[s]

Subscripts

b	bulk value
e	free-stream
rec	recovery
trans	transition of TLC
0	initial state

Superscript

′	differentiation with respect to time

Acknowledgments

I wish to express my deepest graditude to my thesis and academic advisor, Prof. A.F. Mills, for his guidance, patiance and encouragment. His philosophy of researching and teaching real engineering problem initiated and fostered my interest in the field. His kindness towards me and the influence he had during my graduate work will be forever with me. I would also like to express my thanks to Prof. Chang-Jin Kim and Prof. Adrienne G. Lavine for their interest and input by serving as members on my thesis committee.

Financial support provided by NASA Dryden Flight Research Center, monitored by Robert D. Quinn, is greatly acknowledged.

Finally, I am greatly indebted to my parents, James and Ellen, for their support and encouragments through life.

ABSTRACT OF THE THESIS

Design and Testing of an Automated System Using
Thermochromatic Liquid Crystals to Determine
Local Heat Transfer Coefficients for an Impinging Jet

by

Benjamin Tan
Master of Science in Mechanical Engineering
University of California, Los Angeles, 1995
Professor Anthony F. Mills, Chair

Using thermochromatic liquid crystal to measure surface temperature, an automated transient method with time-varying free-stream temperature is developed to determine local heat transfer coefficients. By allowing the free-stream temperature to vary with time, the need for complicated mechanical components to achieve a step temperature change is eliminated, and by using the thermochromatic liquid crystals as temperature indicators, the labor intensive task of installing many thermocouples is omitted. Bias associated with human perception of the transition of the thermochromatic liquid crystal is eliminated by using a high speed digital camera and a computer. The method is validated by comparisons with results obtained by the steady-state method for a circular jet impinging on a flat plate. Several factors affecting the accuracy of the method are evaluated.

Introduction

Accurate methods of predicting temperatures are necessary to effectively cool critical parts and to maximize the lifetime of many high temperature systems. Since failure of most components is a local phenomenon, information concerning local heat transfer coefficients are necessary to determine local temperatures and minimize thermal stress in mechanical components. Conventional methods use an array of temperature sensors or heat flux meters to obtain data necessary to deduce local heat transfer coefficients. To cover a large area, many of these sensors are required. In addition, the accuracy of the results obtained from these sensors depends on whether or not the sensors are able to measure local properties. The spatial resolution that the instrument can achieve is constrained by the physical size of the sensor because the local properties are always averaged over the area of the instrument. In addition, the installation of such instruments and the associated wiring is a highly labor intensive task. Thus, for years experimentalists have sought better and faster ways to determine the temperature distribution on a surface. Thermochromatic liquid crystals (TLC), by their ability to reflect light of a specific wavelength as a function of temperature, can be used to measure surface temperature, and through use in paint form, information over the entire surface can be obtained. Since the physical size of the thermochromatic liquid crystals, even in encapsulated form, is of the order of 20 microns, an excellent resolution of local temperature can be obtained and consequently a more accurate local heat transfer coefficient can be determined.

Alternative methods to determine local heat transfer coefficients.

Traditionally, the method used to determine local heat transfer coefficients on surfaces has been to thermally isolate small segments of the surface and apply a known amount of electrical power to each segment through attached resistance heaters. By measuring the segment surface temperature and associated fluid temperature, the heat transfer coefficient can be determined. To measure the surface temperature of the segment, a thermocouple might be used. The necessary finite size of the thermally isolated segment as well as the finite size of the temperature measurement instrument ensures that the heat transfer coefficients measured are always regional averages, rather than the true local value. Although very fine resolution can be obtained by developing very small instruments, there is a corresponding increase in cost and labor.

The use of a separate heater can be avoided by passing electrical current directly through the surface material. Commonly this has been accomplished by fabricating the surface from thin strips of metal with an insulated backing. Since the electrical resistance varies only slightly with temperature, the local heat flux distribution on each strip is nearly uniform. Thermocouples or infrared temperature measurement devices are used to determine local segment temperature, and detailed determination of local heat transfer coefficients is possible [1]. A uniform heat flux can be attained for flat surfaces, but for curved surfaces, the distortion caused by bending of the heater often results in an unknown thickness with unknown heat flux distribution. This is a problem in that the surfaces over which information about heat transfer coefficient is of interest are rarely flat.

In contrast to the heater elements, the use of melting point surface coatings on the surface is inexpensive, and appears applicable to even the most irregular surfaces. In this method, the surface of interest is sprayed with a thin layer of material

having a precise melting point temperature that can be visually detected. A transient test is conducted in which the surface is exposed to a heated air flow and the melting time at each point on the surface is recorded and related to the local heat transfer coefficient. The capabilities of the method for revealing variations in heat transfer coefficient on complex surfaces have recently been demonstrated [2].

The heat-mass transfer analogy has also been used to determine local heat transfer coefficients for an impinging flow of air by measuring naphthalene sublimation rates. The average coefficient is determined by weighing the naphthalene surface before and after exposure to the air stream. Local coefficients are determined by measuring the resulting change in surface profile with a dial gage[3].

Finally, various types of commercially available heat-flux transducers have been used for convection heat transfer studies for a circular jet impinging on a plate for example, Gardon [4]. This heat-flux transducer, designed to produce an emf proportional to the heat flux over a circular test region with a diameter of 0.9mm (Area=6.36×10^{-7} m^2), was mounted flush against an isothermally heated plate. The small size of the instrument allows subtle details in the local heat transfer coefficients to be resolved, but the labor involved in the installation of the transducer for a curved surface where many transducers and the associated wiring are necessary, makes this method impractical for many applications.

Similar issues of expense and complexity exist when any type of transducer is involved. Also, as the surface geometry of interest becomes more complicated, the difficulty and expense of determining local surface heat transfer coefficient through application of temperature sensors increases considerably. In many cases, the technique becomes essentially impossible to implement. Even if possible, the

expense and labor involved to instrument a single fixed test geometry, might prohibit parametric studies of the effect of geometry changes (which often is of most interest).

As an alternative to some of the more conventional methods to determine local heat transfer coefficients, a transient method making use of the unique properties of thermochromatic liquid crystals will be employed.

Physics of thermochromatic liquid crystals

Thermochromatic liquid crystals were discovered at the end of the nineteenth century. Both Otto Lehmann, a German physicist, and Freidrich Reinitzer, an Austrian botanist, contributed a considerable amount of knowledge to the field and each deserves recognition. The initial observation of the phenomenon was made by Reinitzer in 1888, when he noticed that cholesteryl benzoate had two distinct melting temperatures, a first one at which the solid turned into a milky liquid, and a second at which the liquid becomes colorless. Soon after, Lehmann discovered that the cloudy intermediate phase between the crystalline solid and the isotropic liquid had a crystal-like molecular structure, a phenomenon for which he coined the term "liquid crystal". To assist understanding of thermochromatic liquid crystal behavior, the following section has been extracted from "The HALLCREST Handbook of Thermochromatic Liquid Crystal Technology" [5].

When a crystalline solid with a well defined three-dimensional molecular structure is heated beyond its melting point, it transforms into an isotropic liquid with no molecular structure, and if allowed to cool down, the isotropic liquid reverts back to its original solid crystalline state. However, liquid crystals are unusual substances that do not pass directly from a crystalline solid to an isotropic liquid, and vice versa. Instead, they travel through an intermediate state with molecular order less than that of a crystalline solid and more than that of an isotropic liquid. They possess physical properties of liquids such as fluidity and surface tension as well as optical properties of crystalline solids such as anisotropy to light and birefringence (different index of refraction for different direction of polarization and propagation of light). To a certain degree, this behavior validates the oxymoronic name "liquid crystals" originally coined by Lehmann. An alternative name is "mesophase", which means "of intermediate form".

By exhibiting certain aspects of both solid and liquid phases, thermochromatic liquid crystals have properties that are unique to this intermediate phase. The fluidity allows the liquid crystalline structure to be very sensitive to the changes in the environment, and the resulting structural change alters the optical properties of the amorphous liquid crystal enough to modify the wavelength of the reflected light. A very minor shift in the environment such as changes in electrical or magnetic fields and the presence of trace amounts of chemicals can be noticed by viewing the optical response of the liquid crystal. As a consequence of high structural sensitivity to a change in temperature, liquid crystals can selectively reflect different colors as a function of temperature. These unusual properties are the basis for practical applications, and of particular interest in heat transfer research is the color changing/light modifying property in response to a change in temperature of thermochromatic liquid crystals.

Substances that form liquid crystal phases are generally classified by the degree to which the elongated cigar shaped molecules are ordered. A sematic mesophase, the more ordered of the two classifications, is characterized by the long axes of the molecules being parallel and all neighboring molecules aligned to form very defined layers (Figure 1). In a nematic mesophase, the less ordered of the two, the long molecules remain essentially parallel, but instead of layers of molecules, there is little order with no defined layer, as shown in Figure 2.

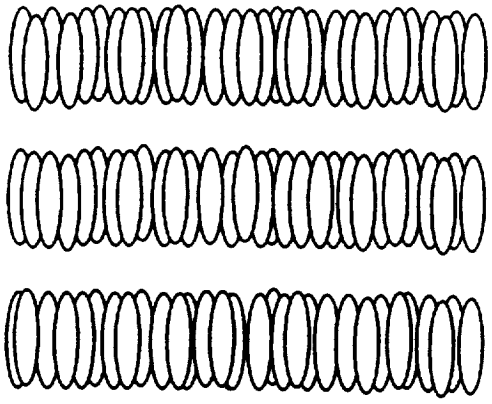

Figure 1. Sematic liquid crystal.

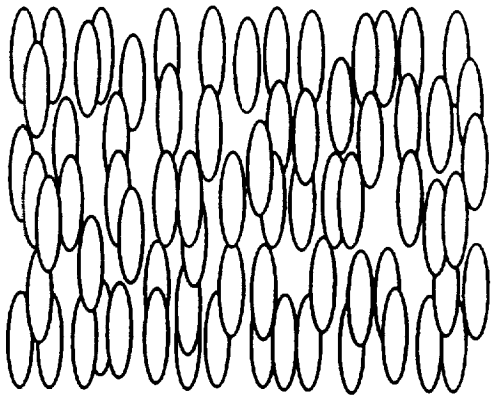

Figure 2. Nematic liquid crystal.

Cholesteric liquid crystal, a sub-class of nematic, exhibits the unique optical properties we normally associate with thermochromatic liquid crystals. The molecular arrangement of this substance is shown with long axes parallel to the plane of the layer (Figure 3). Each layer is very thin, only about 3 Angstrom, and is rotated with respect to its neighbor by about 15 minutes due to the protrusion of a methane chain extending perpendicular to the plane of the molecular layer. Successive rotation of the layers creates a helical pattern along an optical axis normal to the layers.

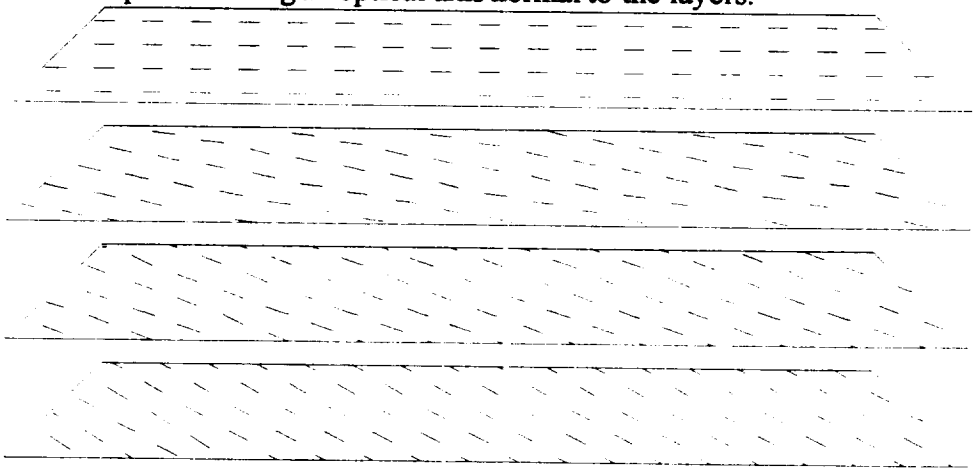

Figure 3. Molecular structure of cholesteric liquid crystal.

Due to their unusual helical structure, cholesteric liquid crystals are optically active, that is the plane of polarization is rotated through an angle proportional

to the thickness of the transmitting material. The first substance to exhibit this property was a derivative of cholesterol: any substance with similar optical property has since been called cholesteric. However, this can be misleading as many optically-active chemicals that are not related to cholesterol or other sterols also show the "cholesteric" liquid crystal behavior. Although the mechanism by which the two types of materials reflect light and change color is the same, it is important to differentiate non-sterol and sterol materials because they exhibit different chemical and physical properties that can be used in different ways to achieve different effects. To differentiate the two types, non-sterol related cholesterics are frequently referred to as chiral nematics.

The pitch along the longitudinal direction of a helical structure of cholesteric and chiral nematic mesophase is of the order of wavelength of visible light. When ordinary white light passes through this sample, the molecular arrangement only transmits wavelength of light corresponding to the pitch of the helix as it continuously turns from one layer of molecules to the next. By changing the pitch of the helix, which can be achieved by changing the temperature of the liquid crystal, the wavelength of the reflected light can be altered, giving liquid crystals the ability to selectively reflect light of specific color in response to a change in temperature.

The selective reflectivity of cholesteric and chiral nematic mesophase can be observed through a number of different textures. The focal conic and planar texture are the most important and they differ only in the degree and direction of the helix in relation to the observer. For focal conic texture, the helical structures are at a 90° angle to incident light. In this form, the cholesteric mesophase scatters light diffusely, and appears milky and not brightly colored when viewed against a dark background. In a planar texture, which can be formed from the focal conic by mechanical shear, the helices are more or less parallel to the axis incident light. This is the texture that exhibits the

unique optical effects usually associated with the cholesteric and chiral nematic mesophase, namely optical activity, circular dichroism and selective reflection of white light to show brilliant colors. Of the two, the properties of the planar texture are those that are normally viewed as being characteristic of the cholesteric mesophase and are the most useful.

The ability of thermochromatic liquid crystals to respond optically to a change in temperature is limited by certain physical phenomena. First, the temperature interval over which the cholesteric mesophase exists is limited at the high end by a transition to the isotropic liquid, and at the low end by a transition to the solid state or the sematic mesophase. Second, the presence or absence of the sematic mesophase plays an important part in determining the color reflecting property of the mixture. When cholesteric mesophase is cooled, the helical structure untwists completely as it undergoes a phase change towards a sematic state. This transformation from helical structure to a planar structure (which occurs over a very short temperature span) causes the cholesteric mesophase to exhibit selective reflection of extremely high temperature dependence. The influence of these pre-transitional effects on the temperature dependence of the reflected wavelength far exceeds that of any other physical or chemical change that the cholesteric mesophase might inherently experience.

Away from the pre-transitional region, the cholesteric structure is also sensitive to temperature changes. Three possibilities exist; the reflected wavelength can increase, decrease or remain unchanged as the temperature increases. These changes can be explained by considering the thermal motion of the molecules comprising the mesophase. As the temperature increases, the thermal motion of the molecules increases resulting in an increase in their molar volume that can affect the helical structure in two opposing ways. The distance between intermolecular layers along the helical axis

increases, tending to increase the pitch and reflected wavelength, or the displacement angle between the long axes of adjacent molecules in the helical stack increases, tending to decrease the pitch and reflected wavelength. In individual chemical compounds the latter usually dominates over the former, and in almost all pure cholesteric and chiral nematic compounds, the pitch and reflected wavelength decrease with increasing temperature. Only a very small change in displacement angle (about one tenth of one degree) causes the reflected wavelength to move from one end of the visible spectrum to the other. This high sensitivity to temperature results in a molecular level structure that is capable of being used as a temperature indicator.

Use of thermochromatic liquid crystals

Thermochromatic liquid crystals (TLC) are very adaptable to measuring temperature in extended areas. There are a number of parameters to be considered when maximizing the accuracy of TLC to measure the temperature. Some suggestions for the use of a cholesteric liquid crystal are as follows:

(1) Since a transient test technique is used, the heat capacity of the thermochromatic liquid crystal film should be small. The heat density of the film material is typically 1.5 J/cm^3. To ensure pronounced transition, a film of 0.02 mm thickness is required. This means that the heat capacity per cm^2 area of the paint is $3x10^{-3}$ J/cm^2. The heat flux from the heated jet to the model being studied should be high enough to ensure that the temperature of the film is increased above the transition temperature of TLC over a very short time period.

(2) To absorb all light and reflect only light due to a change in liquid crystal, the background should be black. This may be done by using a non-oil soluble black paint or black dye. A black dye will allow the black background to be added with little increase in thickness.

(3) The resolution element must be larger than the limit of resolution of the liquid crystal, which is about 0.02 mm. Thus, if the temperature pattern has significant structure below this limit, use of thermochromatic liquid crystal is impractical.

(4) The rate of thermal change in the transient test procedure must be slow enough to allow the cholesteric liquid to reflect the temperature change. The rate of change of color with temperature has a time constant that may be as short as 30 milliseconds.

(5) The temperature of the object to be measured must be in a range where cholesteric materials are available. Liquid crystals of the cholesteric type have been observed

from -40°C to 285°C. However, materials which have been found useful for temperature measurements are presently limited from about 0°C to 120°C.

(6) The surface must be oil resistant. This can sometimes be achieved by use of a water soluble film such as polyvinyl alcohol.

As mentioned before, optical properties of liquid crystals depend on a delicately balanced molecular arrangement. A change of dipole moment or any other disturbance that interferes with the weak forces between molecules result in a dramatic change. Pure liquid crystals, in bulk form, are highly susceptible to environmental contamination, and lifetimes are limited to a few hours if exposed to unfavorable conditions such as chemical vapors, oils, or ultraviolet light. These hazards can permanently alter or remove the color from liquid crystals. In an "office" environment, liquid crystals can be stored on a shelf in a closed closet or bookshelf with little fear of deterioration. A shelf life of over 2 years can be expected. There may be some settling, but stirring or filtering will restore utility to most paints even after long storage.

Liquid crystals may respond to pressure and to shear stress as well as temperature and this should be recognized in choosing the situations for liquid crystal application. The perceived color of a liquid crystal is also a strong function of viewing angle for "bulk" liquid crystal material. These secondary effects are not desired, and most can be significantly avoided by using encapsulated material. Encapsulated thermochromatic liquid crystals are made from a mixture of gelatin and liquid crystal material, precipitated under controlled conditions. The precipitate will consist of spheres of gelatin filled with liquid crystal material, between 5 and 30 μm in diameter. Encapsulation serves the purposes of protecting the liquid crystal from all but the most aggressive environments, and it eliminates the sensitivity to viewing angle. Most commercially available materials are encapsulated.

Thermochromatic liquid crystal applications in heat transfer

Liquid crystals, with their ability to reflect light of specific wavelength in response to a change in temperature, can be used to determine constant surface temperature contours as well as indicate relative hot and cold spots on the surface. With proper calibration of the liquid crystal color temperature response, surface temperatures can be determined. In the simplest application, a thin layer of encapsulated liquid crystals is applied, the system is brought to a steady state, and the observer notes regions of color change and sketches the distribution for the record.

The first reported use of liquid crystals to measure convective heat transfer coefficients was by Venneman and Butefisch in 1973[6]. Heat transfer measurements were reported for a sphere and a sharp cone in a Mach 8 flow. The liquid crystal coated models were quickly inserted into the tunnel and heated aerodynamically by the flow. The color change of the model was recorded using a color movie, and a transient heat conduction analysis was used to extract heat transfer coefficient from the observed temperature-time history. The result agreed with conventional methods using thermocouples.

den Ouden and Hoogendoorn used liquid crystals to measure heat transfer coefficients for jets impinging on a plate in 1974 and 1977 [7]. A glass plate was heated from behind by a constant temperature water-bath and painted with liquid crystals on its front face. A jet of cold air was directed at the exposed face. The heat transfer rate along a visible isotherm was calculated from the thermal conductivity of the glass, using the known temperature of the water bath. A precursor of the modern encapsulated materials was used, in which the liquid crystals were suspended in a solution of polyacrylate resin and solvent.

Liquid crystals were used to directly measure the local heat transfer coefficient using a steady-state method on a heated cylinder by Cooper et al. [8]. Carbon impregnated paper was used to provide a constant surface heat flux, with liquid crystal material deposited on its surface to determine the surface temperature. They also used a segmented coating, with eight different paints, to measure the heat transfer coefficient over a wide range of conditions. The effects of circumferential conduction and radiation on local heat transfer coefficients were corrected for.

Vapor deposited gold on a thin polyester sheet to provide a constant heat flux with liquid crystals used as temperature indicator has been used to obtain accurate local transfer coefficients on a turbine airfoil [9]. The complication of having to attach a heater sheet onto the model was alleviated by the fact that the model was only two dimensional. For the calibration of the liquid crystals, it was recommended that the narrowest color band of the crystal, corresponding to yellow, be used to indicate the isothermal band. To minimize the modification of the color response due to differences between the light source and the camera line of sight, it was recommended the separation angle be limited to 30°. Applying the above method, an experimental error of ±6.2% was estimated, mainly due to non-uniformity in the heater-sheet.

Saabas et al. [11] developed a transient technique to determine local heat transfer coefficients for augmented cooling passages of airfoils. To ensure temporal accuracy for rapid transition of TLC with high rate of heat transfer for augmented surfaces and to remove the human factor in the determination of transition properties, an image analysis system incorporating the use of a video digitizing card, VCR, and a personal computer capable of acquiring 30 frames per second was developed. To minimize the error in determination of transition time, a graph of intensity versus time was developed for selected pixel location on the captured image corresponding to the

desired locations for heat transfer measurements on the surface. The maximum intensity level on the resulting graph corresponds to the liquid crystal in the transition phase, and if the temperature of transition is predetermined, the time to transition and corresponding surface temperature is known for the selected location on the surface. In addition, to account for the variation in gas temperature at the inlet more accurately, a ramp profile for the gas temperature was employed, as opposed to the discrete increase in temperature profile as proposed by Metzger [13]. Errors resulting from the insulative nature of the liquid crystal and the background paint and the validity of the one dimensional heat conduction assumption on augmented surfaces are also discussed.

Baughn et al. [12] compared various aspects of the use of liquid crystals to determine the heat transfer coefficient using both a transient method and a heated-coating method. The latter uses an electrically heated coating to supply a uniform heat flux at the surface, whereas the former transient method involves the use of the convection boundary condition to reduce the raw data to obtain the desired heat transfer coefficient. The differences in the thermal boundary conditions suggest that the two problems are different and therefore may not give the same heat transfer coefficient (particularly for laminar flow). In addition, the difference between the inlet temperature distribution of fully developed parabolic temperature profile of the transient method and the near constant temperature profile of the heated-coating method, as well as host of other differences, ensure that the two problems are different. Nevertheless, the resulting differences in the measured heat transfer coefficients were small and well within the expected errors of the experiment.

Akino et al. [13] developed a method by which multiple isothermal contours can be obtained from a single steady-state heating condition, without the help or uncertainty of human perception. This method uses a set of optical filters having

sharp band-pass transmittance characteristics to extract isochromatic regions, and ordinary light sources having continuous spectral characteristics. Through the use of a black-and-white video camera, the region showing the color with a corresponding temperature, specified by filter, can be observed selectively. In spite of the filters with very sharp band-pass characteristics, the filtered image is not always thin enough to draw an isothermal line directly due to the broad spectral characteristic of the light scattered and reflected from the thermochromatic liquid crystal layer. Thus, with an aid of the digital image processing technique, the isothermal line has to be drawn connecting the local brightest points. The process of connecting the local brightest points was accomplished with an algorithm where pixels of low intensities on the digitized image were successively omitted until only the brightest pixels from which an isotherm can be constructed remained. Then, using a digital tablet, an isothermal line was drawn manually from the remaining pixel. This procedure, though excluding the use of human eye sensation, still requires human aid and is therefore prone to bias in the results.

Kimoto at el. [14] used two kinds of photosensors, namely a red- and a green-light-emitting diode and phototransistor, with an optical fiber to measure the temperature profile appearing on a temperature sensitive liquid crystal film. A red-light-emitting diode with peak emission wavelength of 660 nm and a half-width of 20 nm, and a green-light-emitting diode of peak emission 568 nm and a half width of 25 nm were used. The photosensors were used to precisely measure the surface temperature of the liquid-crystal and subsequently determine the local heat transfer coefficient for a jet impinging on a heated plate. This method was deficient in that the intensity levels collected from the photosensor were point wise, and therefore, the sensor must be repositioned at several locations if good resolution over a large spatial area is required.

In most of the studies summarized to this point, the images were processed for the existence of a single color region that corresponds to a very narrow temperature band. In a majority of the experiments, visual detection of this contour was the most quantifiable description of a single isotherm that could be captured from a single image using a calibrated temperature-color band relation. In some cases, mixtures of different liquid crystals resulting in multiple transitions were used to obtain multiple isothermal lines per image. Camci et al. [15], by implementing a real time hue capturing system (color camera w/ three 8 bit video A/D converters), based on the transient liquid crystal method, was able to capture multiple isothermal lines from a single frame[13]. The color spectrum (hue) appearing on a liquid crystal sprayed surface was calibrated and used to obtain multiple isotherms simultaneously. Using this method, a region of temperature corresponding to a hue and the corresponding heat transfer coefficient were determined. Using this procedure, as many as 40 isotherms and corresponding 40 heat transfer coefficients can be obtained from a single captured frame. The ability to attain 39 additional heat transfer coefficients per frame is unnecessary since the data collected lie approximately in the same area and therefore the value of the corresponding heat transfer coefficients should be the same. For experiments with very high gradients in heat transfer coefficient, a camera with a high throughput could be used to acquire the additional data. In addition, the location and time of transition obtained using intensity-time history, with the aid of a sharp band-pass optical filter, occurs at a very well defined peak, as opposed to hue which is a sloping function. Therefore the lack of distinction in the resulting temperature-hue calibration will not give results that are as accurate as the temperature-intensity calibration.

Wang et al. [16] developed a method (similar to Sabaas) of processing the liquid crystal color change data obtained from transient heat transfer experiments. The

approach uses the full intensity history recorded during an experiment to obtain an accurate measurement of the surface heat transfer coefficient at selected pixels.

Farina et al. [17] developed a video-based system using liquid crystals to make accurate regional surface temperature measurements, independent of the illuminant spectrum, background lighting, angle of incidence, and optical path. The method developed a hue-temperature calibration using a cross-polarized primary lighting and an algorithm to correct for the optical path, the intensities, the spectra of both the primary and illuminant lighting, and noise caused by background lighting. In studies completed under perturbed conditions, the hue-temperature calibrations produced a noticeable inconsistency in comparison with the ideal case. Once the algorithm to correct for the perturbed conditions was applied to the captured image, the discrepancy between the hue-temperature calibration of the ideal and the perturbed condition became more acceptable. The system color calibration, by correcting for the divergent effects of background lighting, allows the hue-temperature system to be used under non-laboratory conditions where the lighting cannot be controlled. In addition, errors resulting from various off-axis lighting/viewing of the crystal on the calibration were presented. It was concluded that to minimize the discrepancy in the calibration, the lighting/viewing angle should be perpendicular to the image.

Chan et al [18] furthered the development of a hue-temperature calibration method and developed a procedure by which the requirement of a linear temperature distribution is omitted. It was concluded that the optimum camera lens aperture (f stop of 2.8) should be used if the sharpest and the most brilliant color image is to be captured. In addition, the use of a tungsten-halogen lamp was recommended for its ability to produce excellent color rendering and to consistently reproduce the same color over its lifetime.

von Wolfersdorf et al [19] developed a hybrid transient step-heating technique using heater foils and liquid crystal thermography to determine local heat transfer coefficients. In this method, heat is applied to the heater foil, which is allowed to heat up beyond the transition temperature of the liquid crystals (as in many of the steady-state methods). A short time after the transition point, the input heat is switched to a lower value. By sufficiently reducing the input heat, the crystal can be made to traverse back to the pre-transition phase. This procedure is a mixture of the transient and the steady-state method, and the solution is only a function of the two times at which the transition occurs, the ratio of the two applied heating and the switchover time. The benefits received from the added complications are that the desired heat transfer coefficients can be solved for without the need to ensure a constant heat flux over the entire surface, and that all complications resulting from liquid crystal color-temperature calibration can be eliminated. The elimination of the need for a uniform surface heat flux solves the difficulties encountered by previous investigators of the steady-state method (especially for curved surfaces), but the entire process of using a surface heat source can be eliminated by employing the transient method. The omission of the color-temperature calibration reduces the amount of work required to conduct the experiment, but this is an achievable task, and by automating the task as has been done by other investigators, the process can be completed relatively easily.

The objective of the present work is to develop a completely automated and expeditious means by which local heat transfer coefficients can be determined. The unique ability of the thermochromatic liquid crystals to change color as a response to a change in temperature will be used to determine the surface temperature during the transient thermal response of a model to a change in fluid temperature. By recording the color response with an image digitizing system and processing the data with a computer,

bias associated with human perception will be omitted. In addition, the temperature of the free-stream will be allowed to increase in time so that the complicated actuators to accomplish a step increase in free-stream temperature will not be necessary. To validate this method, several experiments will be conducted for a jet issuing from a nozzle onto a flat plate and the results compared with those of previous investigators.

Theory

To determine the local heat transfer coefficient using the surface temperature response of a semi-infinite plate will require the analysis of the thermal conduction within the solid. Consider the one dimensional heat conduction in a semi-infinite solid with constant thermal properties and no heat sources. The heat conduction equation reduces to

$$\frac{\partial \theta}{\partial t} = \alpha \frac{\partial^2 \theta}{\partial x^2} \tag{1}$$

If the surface of the solid is suddenly exposed to a fluid stream of constant temperature θ_e and with a constant heat transfer coefficient h_c, appropriate initial and boundary conditions are

$$\theta(x,0) = 0 \tag{2a}$$

$$-k\left.\frac{\partial \theta}{\partial x}\right|_{x=0} = h_c\left[\theta_e - \theta(0,t)\right] \tag{2b}$$

The solution to the stated problem is

$$\frac{\theta(x,t)}{\theta_e} = \operatorname{erfc}\frac{x}{\sqrt{4\alpha t}} - \exp^{h_c x/k + (h_c/k)^2 \alpha t} \operatorname{erfc}\left(\frac{x}{\sqrt{4\alpha t}} + \frac{h_c}{k}\sqrt{\alpha t}\right) \tag{3}$$

To account for a time variation in free-stream temperature $\theta_e(t)$, Duhammel's theorem can be used.

$$\phi(x,t) = \theta_e(t=0)\left[\operatorname{erfc}\left(\frac{x}{\sqrt{4\alpha t}}\right) - \exp\left(\frac{h_c x}{k} + \left(\frac{h_c}{k}\right)^2 \alpha t\right)\cdot \operatorname{erfc}\left(\frac{x}{\sqrt{4\alpha t}} + \frac{h_c}{k}\sqrt{\alpha t}\right)\right] + \tag{4}$$

$$\int_0^t \theta_e'(\tau)\left[\operatorname{erfc}\left(\frac{x}{\sqrt{4\alpha(t-\tau)}}\right) - \exp\left(\frac{h_c x}{k} + \left(\frac{h_c}{k}\right)^2 \alpha(t-\tau)\right)\operatorname{erfc}\left(\frac{x}{\sqrt{4\alpha(t-\tau)}} + \frac{h_c}{k}\sqrt{\alpha(t-\tau)}\right)\right] d\tau$$

At the surface where x=0, Eq.(4) simplifies to

$$\phi(0,t) = \theta_e(t=0)\left[1 - \exp\left(\frac{h_c^2}{k\rho c_p}t\right)\right]\cdot \operatorname{erfc}\left(\frac{h_c^2}{\sqrt{k\rho c_p}}\sqrt{t}\right)\Bigg] + \tag{5}$$

$$\int_0^t \theta_e'(\tau)\left[1 - exp\left(\frac{h_c^2}{k\rho c_p}(t-\tau)\right)\right]\cdot \operatorname{erfc}\left(\frac{h_c}{\sqrt{k\rho c_p}}\sqrt{(t-\tau)}\right)\Bigg] d\tau$$

If the temperature at a point of interest on the surface can be measured for one time and the fluid temperature as a function of time is known, Eq.(5) can be solved iteratively to determine h_c.

Experimental apparatus, data acquisition, and data processing

A schematic drawing of the apparatus is shown in Figure 5. Specifications of each item are given in Appendix D. High pressure air from the building supply was used as the working fluid. A pressure regulator was installed to maintain a constant mass flow rate when the required high flow rates exceed the capacity of the building air system to maintain a steady supply. Centrifugal filters were installed on both the upstream and downstream sides of the pressure regulator to remove any excess moisture resulting from expansion and the impurities that might be present in the air supply. Further downstream, a turbine flowmeter and a pressure transducer were installed to determine the volumetric flowrate of air. To heat the air, a 1,625 W resistance heater was used. A variac is used to control the power input and hence the air temperature. Forty gage copper-constantan (Type T) thermocouples with exposed beads were installed to measure the temperature of air immediately downstream of the turbine flowmeter and at the exit of the nozzle, as well as the initial temperature of the test plate. All analog signals generated by the instruments were transmitted to and digitized with a Strawberry Tree MINI-16 data acquisition card mounted on an IBM compatible personal computer.

The dimensions of the test plate are 20.32cm x 22.86cm x 1.27cm (8" x 9" x 1/2"). Care was taken to properly apply the TLC, because a thick or uneven application causes systematic and random errors in the results. An artist's type airbrush using a constant 30 psig air source provides a good means by which the crystal could be applied onto the surface. Propellants from a canister should be avoided since the pressure of the supplied gas from such a device drops quickly with use, making it difficult to evenly coat the paint on the surface. A thin layer of encapsulated TLC was

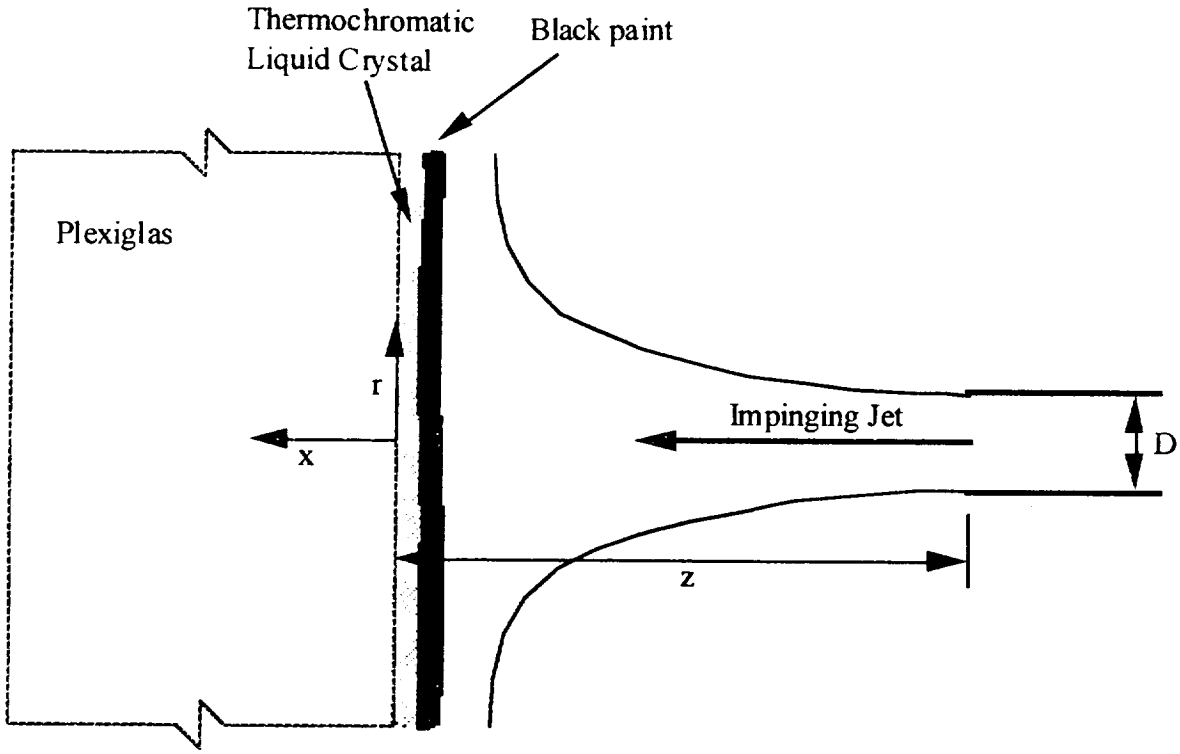

Figure 5. Close caption of the impinging jet showing to coordinate system.

sprayed with air brush positioned approximately 25 cm away from the model. The paint was allowed to dry, and several additional coats were applied to achieve a high gloss finish. To enhance the brilliance of the liquid crystal during the transition phase and to eliminate the background light which transmits without modification through the opaque or sometimes transparent liquid crystal during the non-transition phase, the backside of the TLC was covered with a thin layer of water based black paint. In each step of the application of the TLC and black paint, precautions were taken to ensure that the front side of the Plexiglas was not damaged in any way, so as to avoid scratches that might appear as erroneous transition points in the digitized image.

Due to the highly transient nature of this experiment, reliable results can only be attained if an accurate time-temperature transition relationship (usually more demanding than human perception can provide) is obtained. In addition, to remove any

bias resulting from human involvement, a Charge Coupled Device (CCD) camera connected to a digital image acquisition system was employed to digitize the transition process of the liquid crystals and to determine the corresponding time of transition. With the image capturing system capable of acquiring as many as 30 frames per second, the time and the location of the liquid crystal transition relation for surface temperature measurements can be quantified very accurately. The resolution of image is 640 x 480 x 8 bit pixels. The CCD camera is sensitive to the energy content of the reflected light from the liquid crystals and relays the information to the image digitizing card in units of voltage corresponding to the energy level of the reflected light. The image digitizing card scales the voltage to numerical values from 0 to 255, with 0 being absence of light and 255 being complete saturation with light.

The ability of the image capturing system to distinguish the transition location from the non-transition locations by examining the energy level of the reflected light can be greatly improved by applying a very narrow band-pass optical filter directly in front of the camera. This filter, by allowing only light of selected wavelength (the wavelength corresponding to the transition color) to pass through and absorbing all other wavelengths, enhances the difference in energy intensity corresponding to the liquid crystals in transition and others that might only be tending toward transition. In most previous studies[7,9], it was decided that the visual detection of the yellow contour provides the narrowest region from which the location of the transition can be determined. However, for reasons of availability of a red filter and the possibility of further improving the transition detection by also emitting light of specific wavelength from the source end with the application of a red laser, the recommendation of using a yellow filter was disregarded. The filter was effective in minimizing the intensity of non-transition colors, with minimal effect on the intensity of the red portion of the

visible light spectrum. This procedure provides an even sharper transition point and thus a more accurate method of determining the transition point.

As mentioned earlier, the possibility of emitting a light of very specific wavelength at the source side was considered (as opposed to the use of halogen-tungsten or incandescent light source as previously done by other investigators). This was implemented with the use of a He-Ne laser, which has a very narrow band-width. The idea is that by emitting light of very specific wavelength at the source, only the specific wavelength corresponding to the wavelength of the emitted light will be likely to be reflected back. Several problems resulted from this method. In particular, it was difficult to get adequate dispersion of the laser beam without getting any interference on the illuminated light source. Various types of defocusing lenses were used but none was successful in that the defocused laser beam must travel through the air, which causes a destructive interference in some places and constructive interference in others.

As an alternative to using a small laser beam to aid in the detection of transition point, a recommendation made by other investigators of using a light source with a continuous distribution of energy from the entire spectrum of visible light was considered. When a standard incandescent light bulb was used, the intensity level of all colors on the digitized image was magnified thus making it easier to visually determine the location of maximum intensity more easily. One difficulty when using a directed light source is that the location of maximum intensity changes depending on the relative positions of the light source and the camera to the object. It was suggested by previous investigators[19,24] that the wavelength of the scattered light depends on the angle of incidence of the source as well as that of the observer, leading to a skewing of the image received by the camera. This effect is the greatest when the light source is at an oblique angle. To minimize the deviating effect of the scattered light, it was suggested that the

light source and the camera be positioned such that the direction of illumination and observation coincide. In addition to the problem of how the crystals scatter light, the heat generated by a strong incandescent light source may cause the liquid crystals to undergo transition prematurely.

Image acquisition and digitization

Once the image has been captured and digitized by the video system, it is necessary to store the image in memory so that analysis can be applied after the experiment is completed. To store a single frame of 640 x 480 x 8 bit data requires approximately 0.3 Megabytes of memory, and storing a large number of frames can add up to a very large memory requirement. The Data Translation 3851 image digitizing card has 1 Megabyte of onboard memory that can be accessed very quickly. In addition, the computer is outfitted with 32 Megabytes of RAM that can accommodate all the images necessary, but is limited in speed by the bottleneck at the transfer of data from the memory on the image acquisition card to the RAM on the main CPU.

The importance of speed is more crucial near the beginning of the experiment because the transition of the TLC near the stagnation point occurs very quickly due to the very high heat transfer coefficient. For this region, the speed at which images can be stored can be increased by capturing less than a full frame. Since the stagnation point corresponds to a small image area, it is possible to achieve the needed speed increase without losing any relevant information at the beginning of the experiment. In the region away from the stagnation point, the area over which pertinent information exists is larger, but the corresponding transition rate of the liquid crystal is also slower due to the lower convection coefficient. Therefore, far from the stagnation point, we can acquire larger images at a slower rate without overlooking crucial events in the transition of the liquid crystals. The use of a variable size image for a circular jet impingement experiment allows all necessary information to be stored at an acceptable rate. However, when different nozzle shapes are considered, such as a slot nozzle, it may become necessary to modify the image capturing system to increase the rate at which the information can be stored.

To maximize the speed at which images can be acquired in the earlier part of the experiment, the Megabytes of general purpose memory available on the Data Translation board is used as opposed to slower main memory available on the mother board of the computer. If necessary, the 1Mbyte of memory available on the DT board can be increased to 8 Mbytes. Once the fast memory on the DT board has been occupied, the slower memory available on the mother board can be used to store the additional data. This reduction in speed by using the RAM on the CPU is significant, but as mentioned earlier, fast acquisition is no longer crucial due to the slower transition rate of the liquid crystals in the later part of the experiment.

Image processing to determine transition

Once the images have been digitized, some processing of the images is necessary to determine the location at which the transition occurs. Firstly, the intensity of the original image (before any crystals have been activated) was subtracted from all later images where the crystals have been activated. This ensures that any small blemishes on the Plexiglas will be negated, and not be mistaken for an erroneous transition region. Once all the intensity of the images in transition have been subtracted, several options were studied to determine the most accurate method to locate the transition points. A series of common edge detection methods such as the Laplacian edge detection and smoothing technique, in combination with an image sharpening technique, were considered. These had limited success because of noise in the digital signal, and because the transitions of isochromatic contours corresponding to temperatures were gradual, making the edge detection algorithm ineffective. In addition, the assumption that the pixel with maximum intensity corresponds to the location red transition, to indicate the transition point was considered. This method of simply finding points of maximum intensity has been used by previous investigators[12], and gives reasonable results. However, the resulting contours are a slight function of the location of the light source and, as the angle of the incidence light changes, the isochromatic contours are deformed. Also, the resulting contour was somewhat scattered and discontinuous.

The possibility of following the contour corresponding to the local maximum intensity was considered. Due to noise from the A/D converter and minute imperfections in the crystals during application, small but still discernible errors appeared in the digitized image. To the human eye, the small perturbations were not apparent, but when we wish to determine the path of local maximum intensity using the

computer, the smallest noise in the image causes the contour to diverge from the contour that was obvious. Several different algorithms were tested to resolve this problem. One such algorithm was to use the sum of the intensity formed by the matrix of some size as a criterion to determine the next location on the contour that corresponded to the maximum sum. This method was somewhat unreliable because the resulting contour was not unique, and sometimes the contour would enclose smaller contours due to the noise in the digitized image.

The most consistent method that did not have the above problem is when the vector used in the summation was limited to the vectors in the current direction and two others directed slightly to the left and slightly to the right of the current direction as shown in Fig. 6, . This limited the amount that the vector direction could change at any one time; the method worked consistently and the resulting contour was smooth.

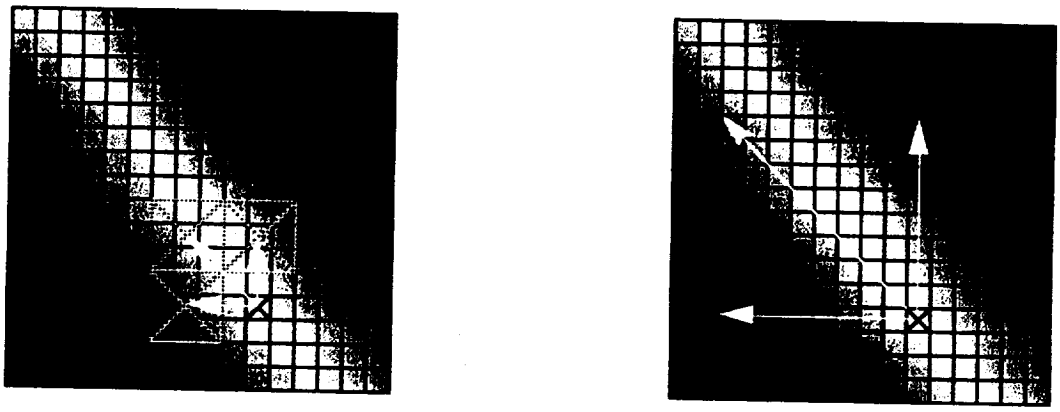

Figure 6. Pictorial representation of contour following method.

The above method gives adequate quantitative results and by providing an image of the contour of constant heat transfer coefficients, it is suitable for qualitative heat transfer studies. For heat transfer studies with quantitative results as the final goal, improved results can be achieved by considering the time history of the TLC for selected locations on the test plate. In doing so, each individual image is treated as a temperature

transducer with the capability to indicate the surface temperature for a single instante in time. By acquiring only a few data points, the throughput of the image capturing system can operate near its maximum speed (30 frame/sec), and the slow task of having to save large amounts of image data in memory is avoided. In addition, the analysis requires only the location and the corresponding time of TLC transition. By having the user define the x-y location of interest ahead of time and using the image capturing to determine the time of the transition, the information of interest is acquired quickly, as well as gaining the added benefit of having the number of the unknowns reduced from two in space to one in time. This simplifies the data reduction as well as improve the location and time correspondence of TLC transition by allowing for an increase in data acquisition rate. A sample graph of the intensity vs. time for various locations is provided in Fig. 7.

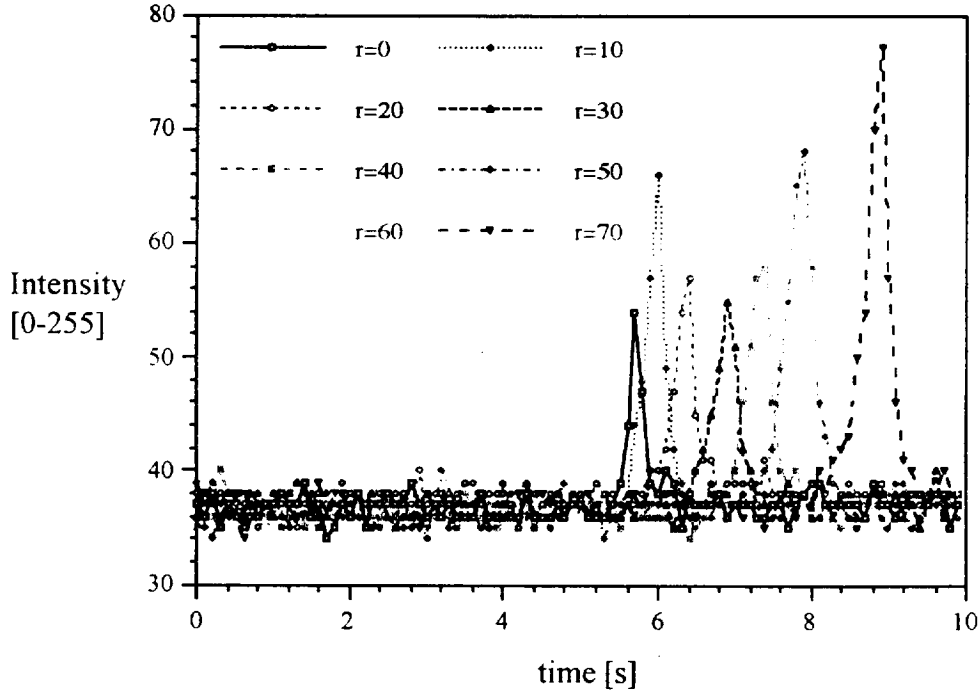

Figure 7. Intensity vs. time for selected pixel locations.

From the graph, the time of transition can be easily selected for a given x-y location due to the very well defined peak intensity shown in the intensity vs. time history graph. The issue of high level of noise that complicates the determination of transition location from the intensity vs. x-y location graph was mostly nullified by the very well defined peak intensity.

Validation of the technique

A highly automated and computer driven technique has been developed to experimentally determine heat transfer coefficients. The unconventional nature of the technique makes it necessary to validate it through comparisons with experimentally obtained data using established methods, and by careful error analysis. The first experiment performed was at Re≅23,000, and z/D=6 in order to make a comparison with results obtained by Baughn [20,21] using a steady-state method with conventional sensors. The results are shown in Fig. 8.

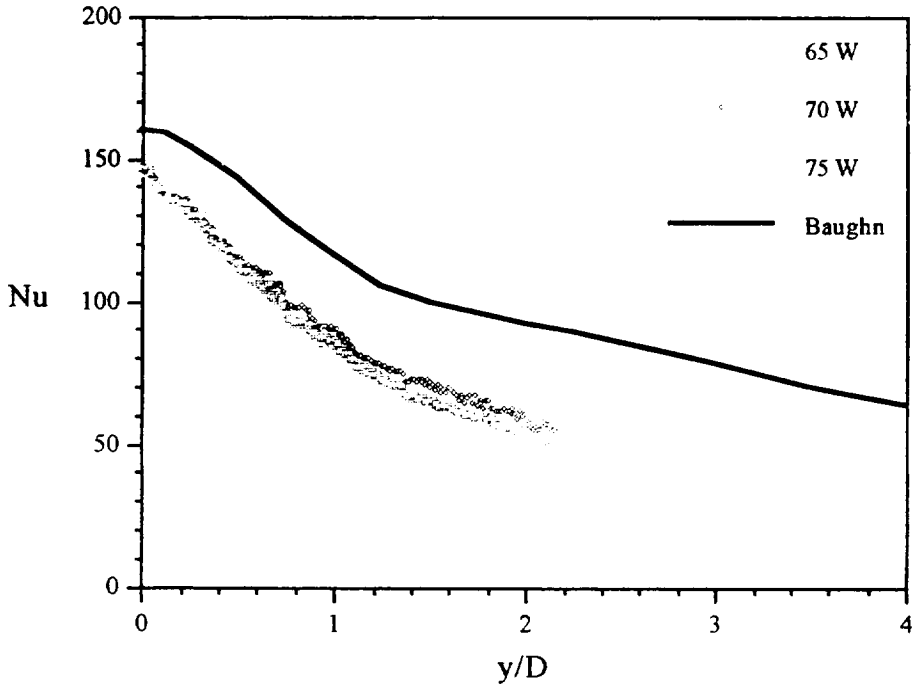

Figure 8. Comparison of measured Nusselt number distribution with Baughn [20,21]; Re≅23,000, z/D=6.

Near the stagnation point, the Nusselt number was about 7% lower than that of Baughn and the difference increases for locations away from the stagnation point. The lower Nusselt number over the entire range can be attributed to the entrainment of the hot air

into the cooler ambient air. For a fully turbulent jet (Re > 3000), the length of the jet's potential core has been measured to be about 6 - 7 nozzle diameters[44]. The potential core is defined as the region of the jet where the centerline velocity of the jet is not reduced by entrainment of ambient into stagnant air. For the case of a heated jet, where the temperature of the jet can reach as high as 60°C, the density of the jet can be as much as 20% lower than the density of the ambient air at 20°C. This lower density air is less effective in penetrating the stagnant air at a higher density, and therefore is more susceptible to the effects of entrainment. The shorter potential core expected for this case of a heated jet entraining into colder air results in a jet with lower effective velocity reaching the plate, as opposed to the case of a jet entraining into surrounding air of similar density. In addition, the diffusion of heat due to vortex exchange between the jet and the surrounding air in a free turbulent jet can be twice as effective as the diffusion of momentum, also causing a reduced jet temperature reaching the plate. These two effects combined can account for the lower stagnation Nusselt number measured. Furthermore, as the jet travels further downstream (away from the stagnation point), the effects of the entrainment become more significant and therefore the reduction in Nu becomes greater.

To omit or at least limit the effects of entrainment, the plate was positioned two diameters downstream of the nozzle exit. Nine different tests were conducted for a range of Re and three different heating rates. The three different heater settings were selected in order to study the effects of free-stream temperature on the accuracy of the experiment. Through the duration of the nine experiments, the relative position of the plate, the nozzle and the CCD camera were not altered. This ensured that the same region of encapsulated TLC and the sensors of the CCD camera were used to obtain the surface temperature for a given x-y position on the impinging plate. The results are shown in Figs. 9a-c.

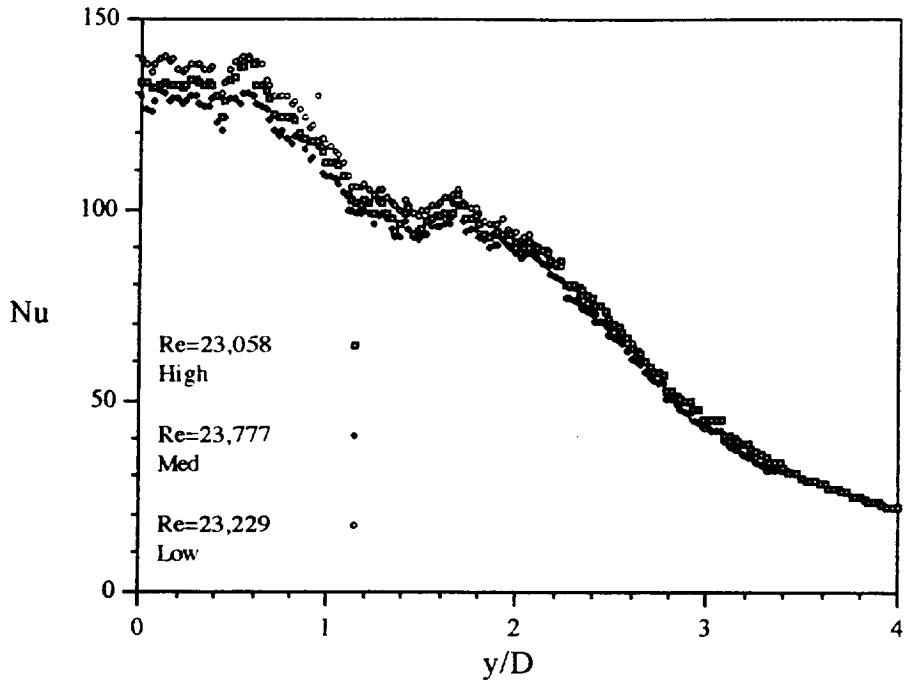

Figure 9a. Nusselt number distribution for three different heating rates: Re≅23,000, z/D=2.

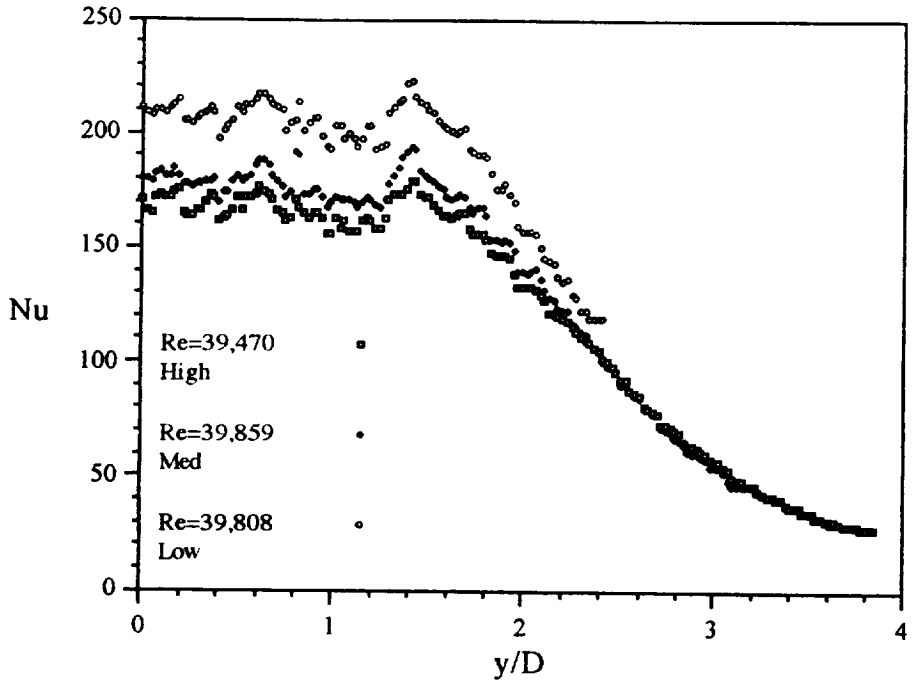

Figure 9b. Nusselt number distribution for three different heating rates; Re≅40,000, z/D=2.0.

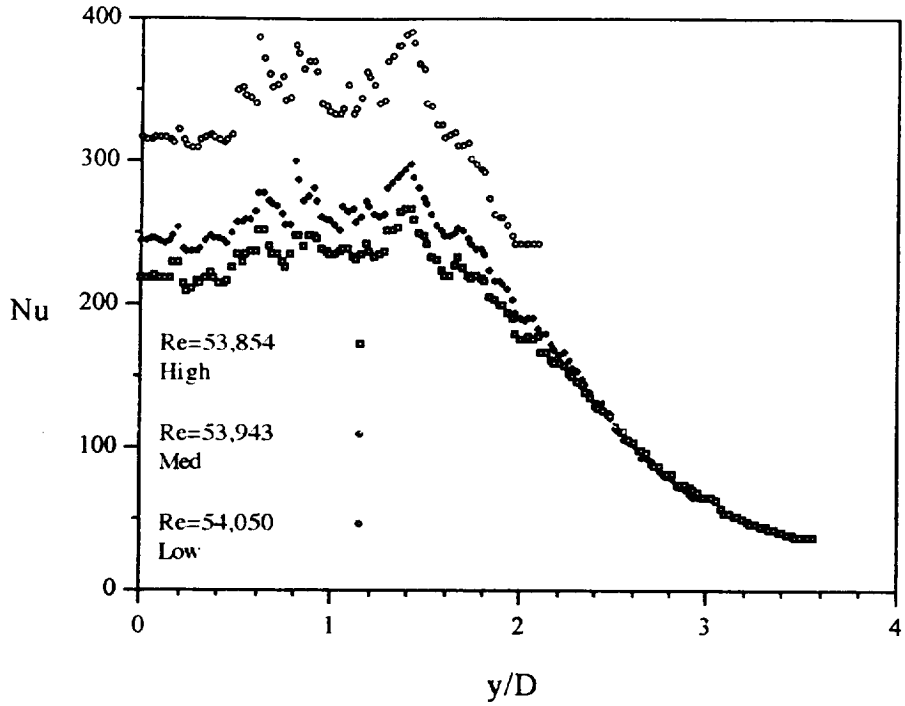

Figure 9c. Nusselt number distribution for three different heating rates; Re≅54,000, z/D=2.0.

Local spatial variations in the Nusselt number distribution can be observed, and are consistently at the same y/D location for all nine experiments. Since the same encapsulated TLC were used to obtain the same local surface temperature, the disturbance of Nusselt number distribution for a given y/D location must be caused by an imperfection in the application of the TLC and/or black background paint. Using a 500X microscope, the surface uniformity of the paint on a microscopic level was investigated. For a given point on the surface, peak to valley distances of up to 50 microns were measured. An improved method for the application of the paint must be considered.

In addition to the local variations, the Nu distributions for the lower heating rates are shifted upward for Re≅40,000 and Re≅54,000. For the Re≅23,000,

variations in heating rate did not affect the Nusselt numbers. The discrepancy in the Nusselt number due to the different heating rates can be explained by considering the air temperature at the nozzle exit over the duration of the experiment. Figure 10 shows the temperature as a function of time superimposed with the free-stream temperature at the time of transition for various Re at the low and high heating rates.

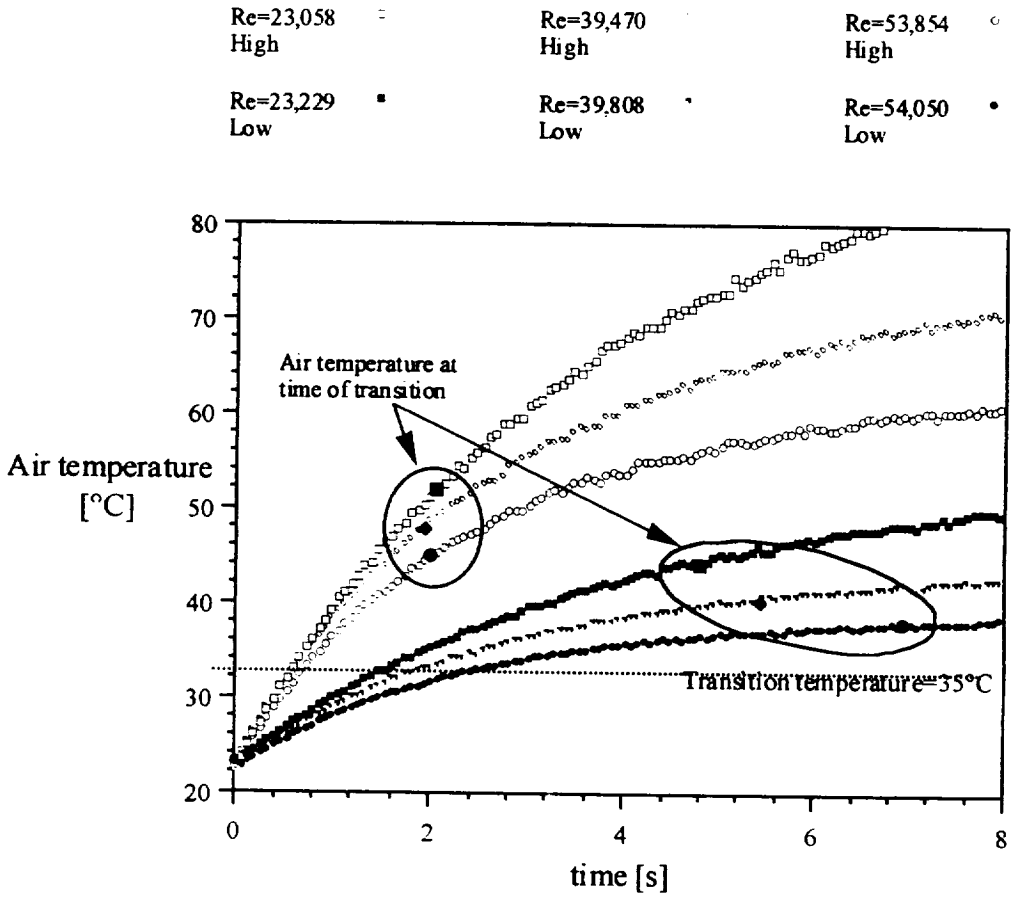

Figure 10. Air temperature vs time for various Reynolds numbers and heating rates.

For the high heating rate, the air temperature at the time of transition is well above the transition temperature of the TLC, ensuring that any marginal uncertainty in the temperature measurement is insignificant. However, for the low heating rate, the temperature of the heated jet was marginally above the transition temperature of TLC,

requiring more accurate temperature measurements for good results. In particular, a correction must be made for an increased air temperature due to kinetic energy being transformed into thermal energy. Assuming a recovery factor $r=Pr^{1/3}$, a new set of Nusselt number distributions were obtained, and are presented in Figs. 11a-c.

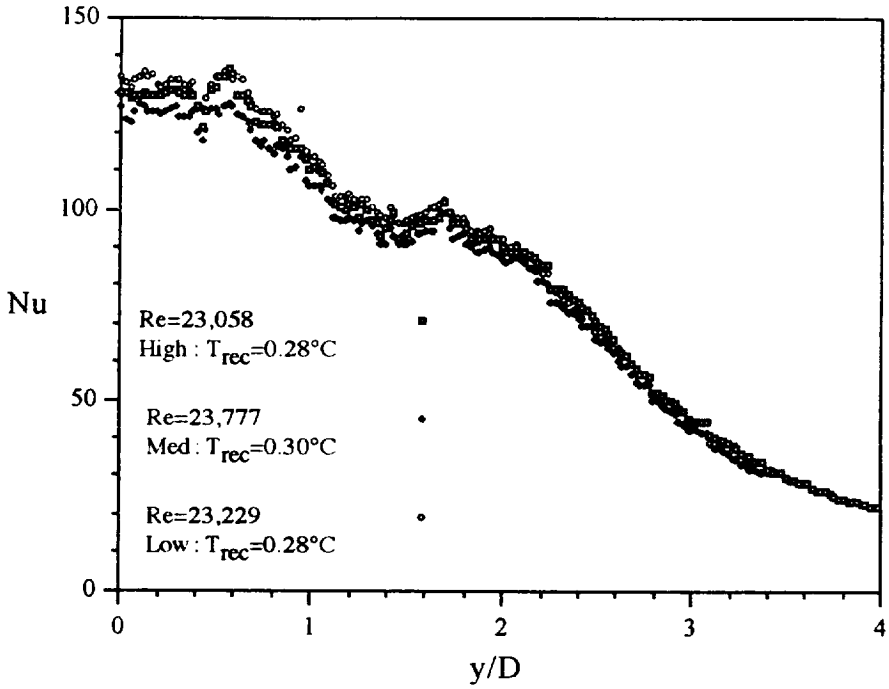

Figure 11a. Nusselt number distribution for three different heating rates accounting for recovery temperature; Re≅23,000, z/D=2.0.

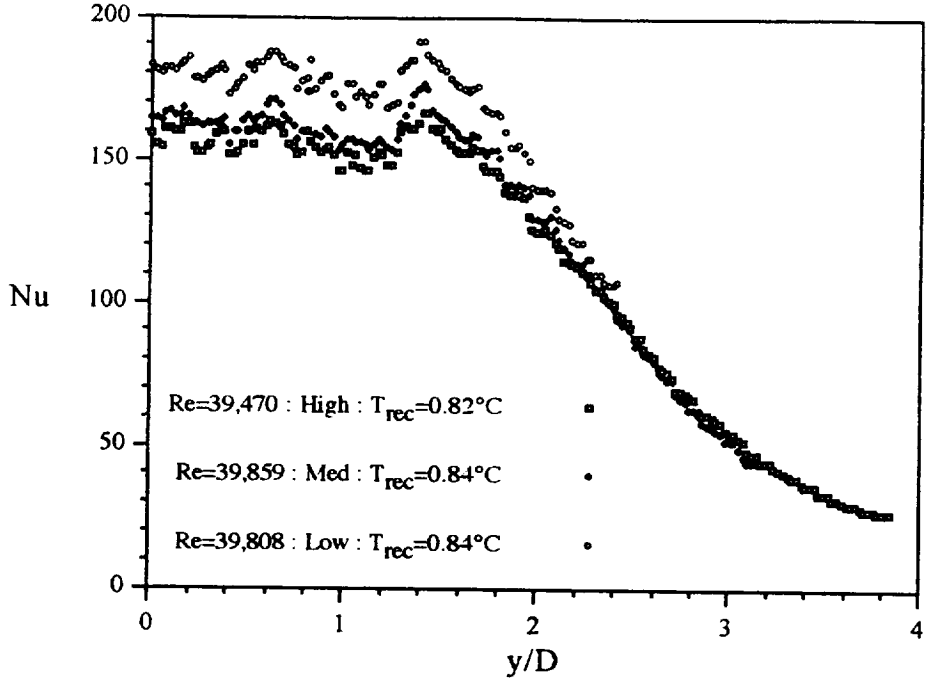

Figure 11b. Nusselt number distribution for three different heating rates accounting for recovery temperature; Re≈40,000, z/D=2.0.

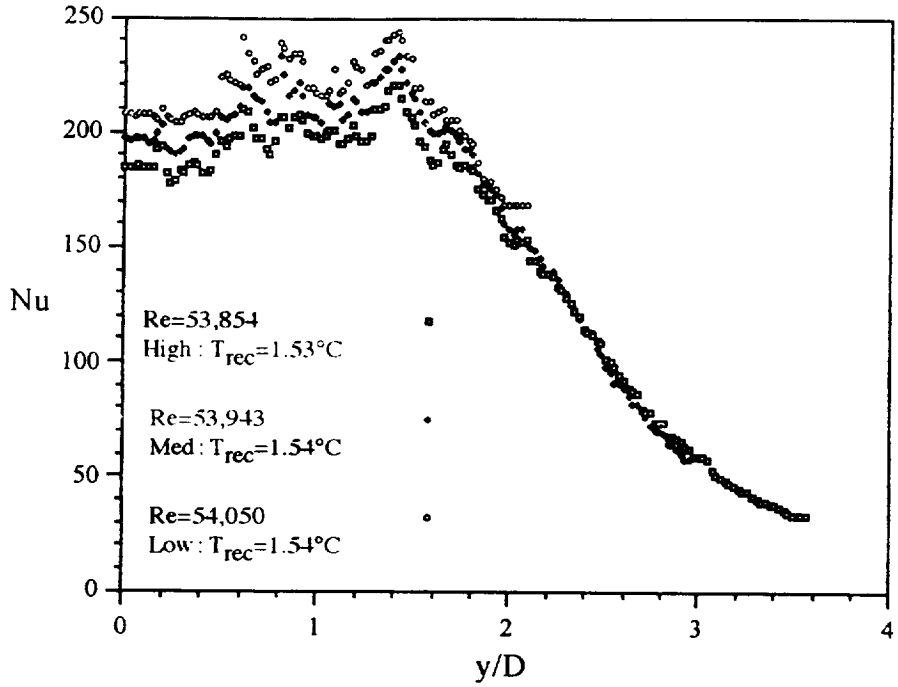

Figure 11c. Nusselt number distribution for three different heating rates accounting for recovery temperature; Re≈54,000, z/D=2.0.

After accounting for the recovery factor in all three set of Reynolds numbers, the Nusselt number distribution for both the low and the medium heating rates approached that of the high heating rate. However, for many flows the recovery factor is not precisely known. The need to consider the increase in air temperature due to viscous dissipation as well as other errors associated with air temperature measurments which might esculate to larger errors in the calculated Nusselt number can be completely avoided by ensuring that the free-stream temperature is comfortably above the transition temperature. In a similar manner, any errors associated with other temperature measurements, such as the initial temperature of the plate, will also be minimized by conducting experiments at the higher temperatures.

To continue the validation of the TLC technique, the Nusselt number from the current method was once again compared with Baughn's results. In Fig. 12,

Baughn's results from two different sources differ slightly for the region near the stagnation point. The difference occurs near the stagnation region in that the earlier of the two studies has a flat plateau extending from the stagnation point to 0.6 diameters downstream, while the later study shows a sloping distribution with Nusselt numbers unspecified for locations near the stagnation point. The only changes in Baughn's methods that can be determined from the publications is the addition of a heater, a different test plate, and a correction for heat loss due to radiation. The change that could have altered the Nusselt number distribution as described above is not apparent.

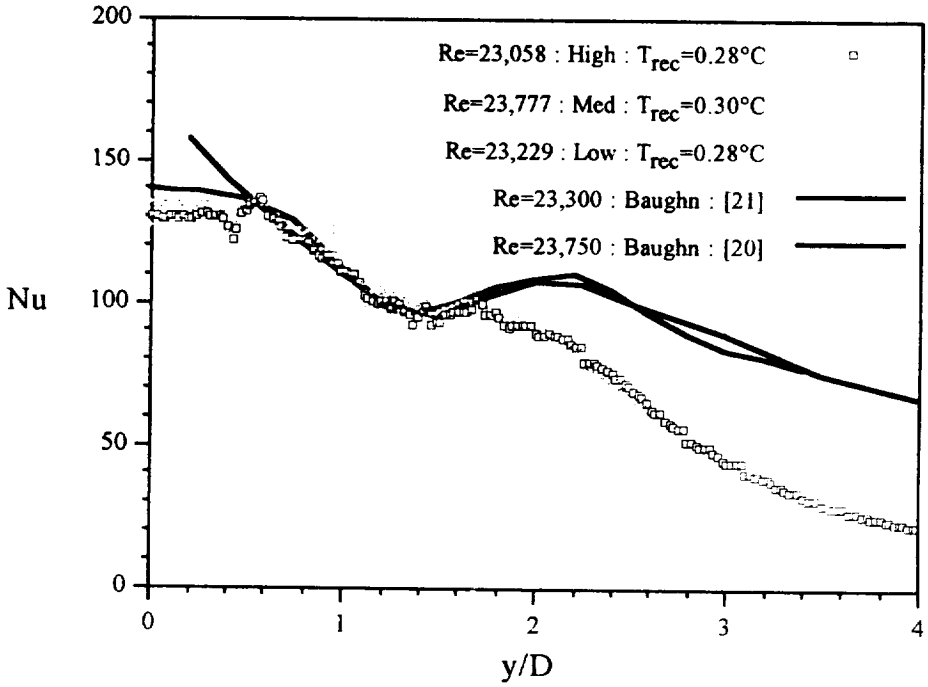

Figure 12. Comparison of measured Nusselt number distribution with Baughn [20,21]; Re≅23,000, z/D=2.0.

Excluding the discrepancy near the stagnation point, the results are almost identical for the region less than 1.7 diameters downstream of the stagnation point. However, beyond that point, the mixingof the outer portion of the jet with ambient air reduces the

ability of the heated jet to transfer the energy to the plate, and lower values of Nusselt number result.

With good agreement in the region for which the comparison is legitimate, the sensitivity of the Nusselt number resulting from uncertainties in various parameters affecting the Nusselt number will be discussed, such as the TLC transition temperature, thickness of black paint and TLC, lighting conditions, and thermal properties of Plexiglas.

Sensitivity of Nusselt number to uncertainty in surface temperature at transition

For a transient situation with the free-stream temperature increasing as a function of time, the relative importance of the surface temperature is difficult to characterize. Therefore, using four representative free-stream temperature profiles, the error in the stagnation Nusselt number was determined for an estimated uncertainty in the TLC transition temperature. The results are shown in Fig 13.

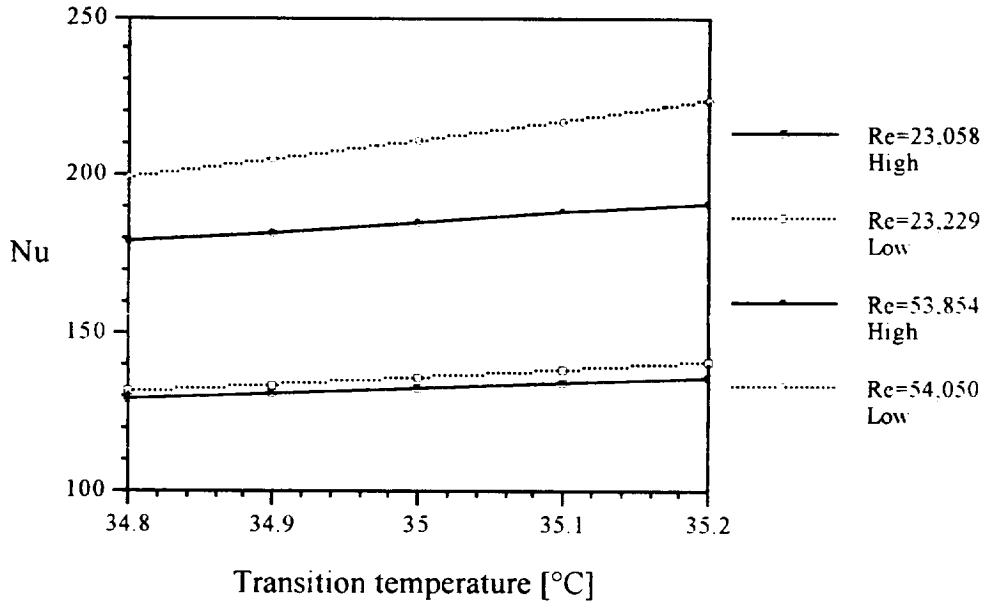

Figure 13. Stagnation Nu vs. TLC transition temperature for various Reynolds numbers and heating rates.

For the trial with Re≅23,000, the errors in the stagnation Nusselt number due to ±0.1°C uncertainty in TLC transition temperature (nominal value 35.0°C) was ±2.7% and ±3.0% for the low and high heating rates, respectively. For Re≅54,000, the errors were ±3.2% and ±5.9% for the high and low heating rates respectively. The increase in Nusselt number dependence on the TLC transition temperature for the low heating rate could again be attributed to the lower temperature difference between the free-stream air and the surface.

Sensitivity of Nusselt number to the thickness of black paint and TLC

With the addition of the black background paint of finite thickness, the TLC no longer measures the surface temperature, but instead the temperature at paint-TLC interface. To examine the relative signifiance of the systematic error caused by the addition of the black paint, it was assumed that the TLC and the black background paint had similar thermophysical properties to those of the Plexiglas. Results for a range of paint thickness are shown in Fig. 14. From the graph, the sensitivity of stagnation Nusselt number for a given paint thickness increased with heating rate for both Re≅54,000 and Re≅23,000. To explain this phenomenon, consider the in-depth temperature profiles determined at the TLC transition time shown in Figs. 15a-c for the different heating rates. For all three Reynolds numbers, the slope of the temperature near the surface was steepest for the high heating rate. As the heating rate increases, so does the temperature gradient at the surface at the time of transition. The amount of paint thickness is difficult to determine but, for a given thickness, the degree to which the surface temperature deviates from the measured temperature will be greatest when the temperature profile is steepest. And as shown in Fig. 14, the sensitivity of the Nusselt number to the thickness of the paint is always greater for the case with the higher of the two heating rates.

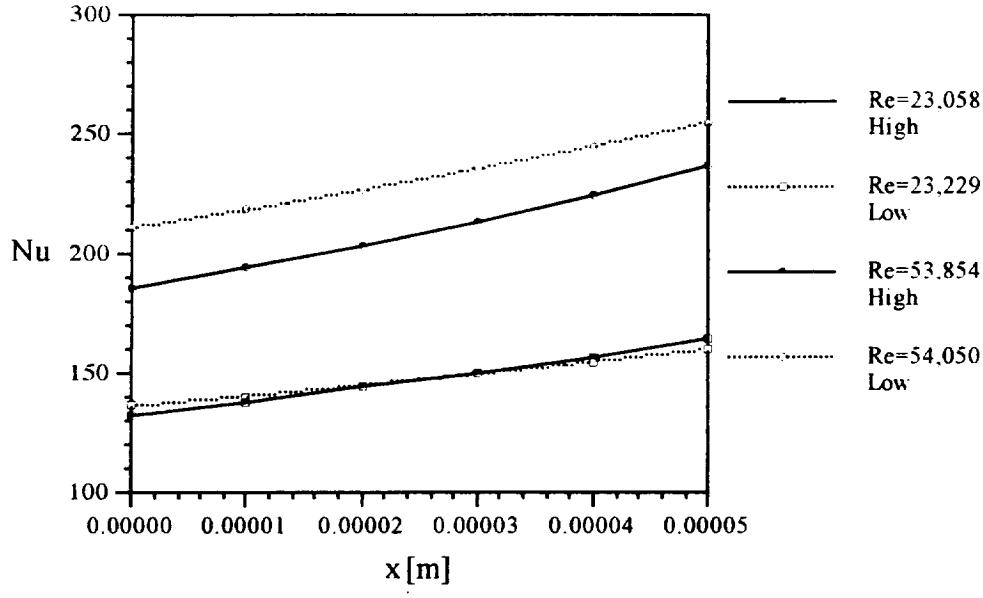

Figure 14. Stagnation Nusselt number vs. thickness of TLC and black paint for various Reynolds number and heating rates.

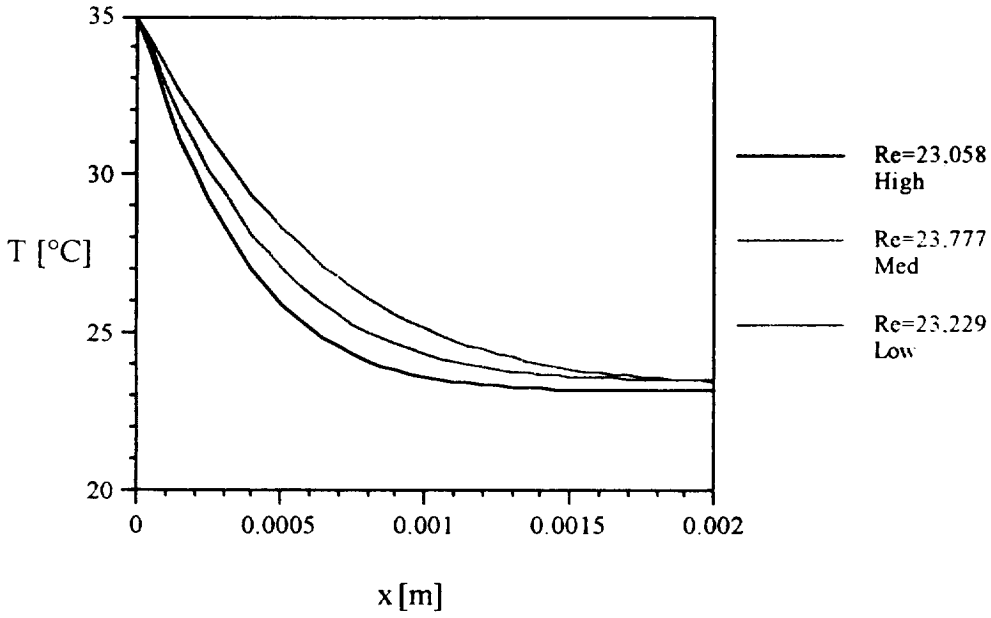

Figure 15a. Temperature vs. depth at the stagnation point and the time of transition; Re≅23,000, z/D=2.0.

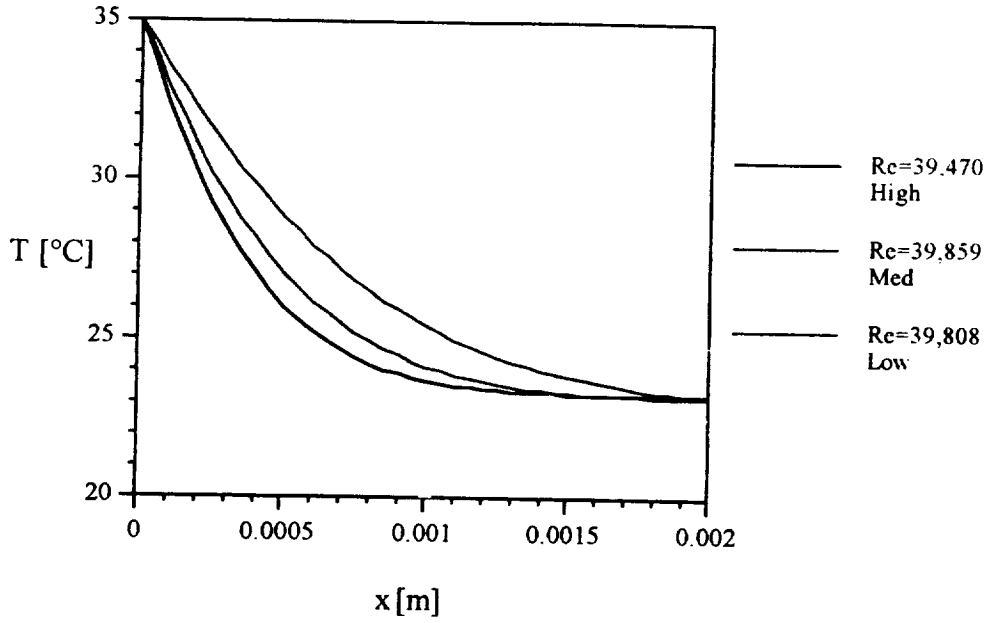

Figure 15b. Temperature vs. depth at the stagnation point and the time of transition; Re≅40,000, z/D=2.0.

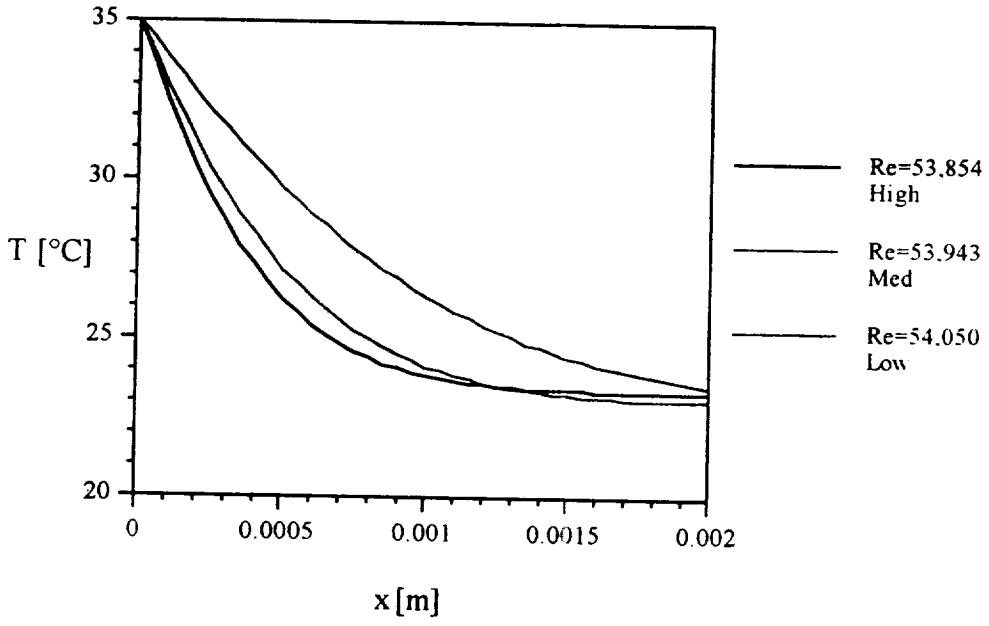

Figure 15c. Temperature vs. depth at the stagnation point and the time of transition; Re≅54,000, z/D=2.0.

Sensitivity of Nusselt number to different lighting conditions

All experiments were conducted under typical fluorescent lighting with a 300 W halogen light to aid in the detection of the TLC transition. Continuing use of the 300 W halogen as the main light source, various combinations and positions of the secondary lights were used to give some indication of the effects of lighting conditions on the color response of the TLC.

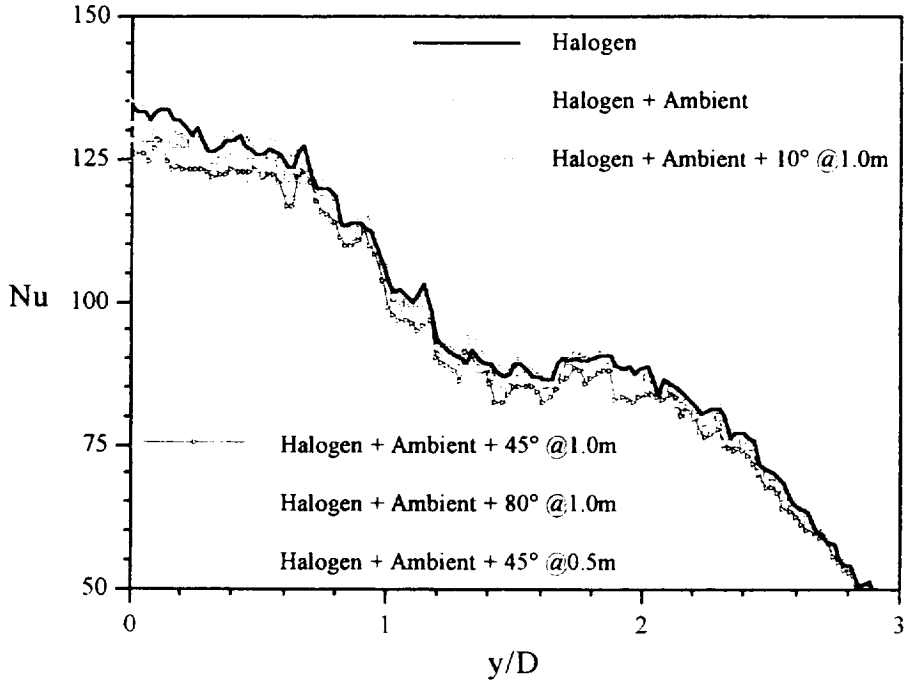

Figure 16. Nusselt number distribution for various lighting conditions.

In Fig. 16, the stagnation Nusselt number is seen to deviate by about ±7% from the mean value. The deviation was fairly random with no reasonable physical explanation for the Nusselt number dependence on lighting condition. The discrepancy in the Nusselt number is not greater than the expected repeatability of the experiment.

Sensivity of Nusselt number to the thermal properties of Plexiglas

To determine the Nusselt number, the necessary thermal properties were compiled from the manufacturer, but uncertainties in the values were not available.

Therefore, the sensitivity of Nusselt number to uncertainty in the various thermal properties was determined. In Figs. 17 and 18, the errors in Nusselt number due to a percentage change in $\alpha_{Plexiglas}$ and $k_{Plexiglas}$ are shown.

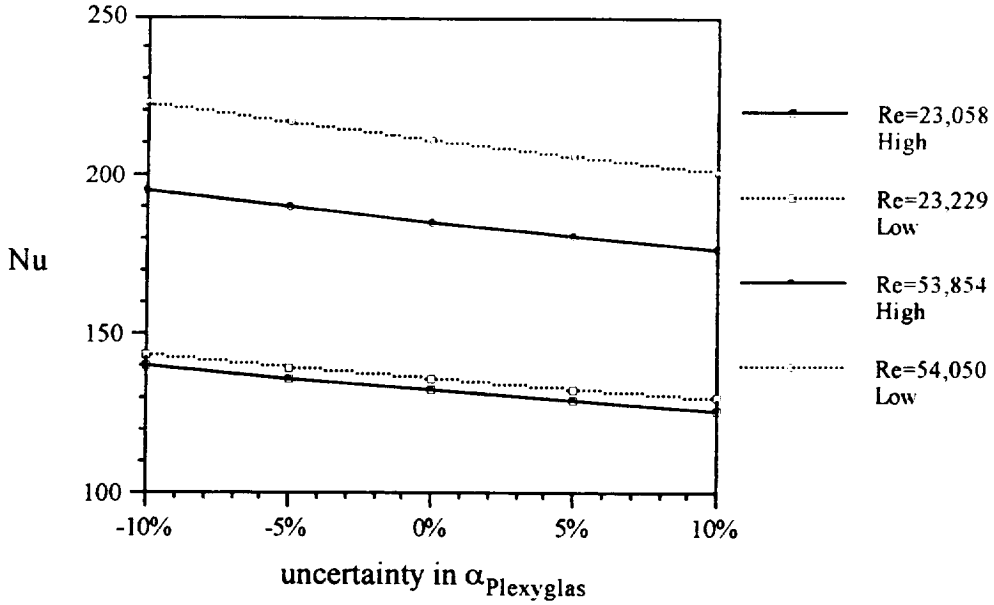

Figure 17. Stagnation Nusselt number vs. uncertainty in thermal diffusivity of Plexyglas for various Reynolds number and heating rates.

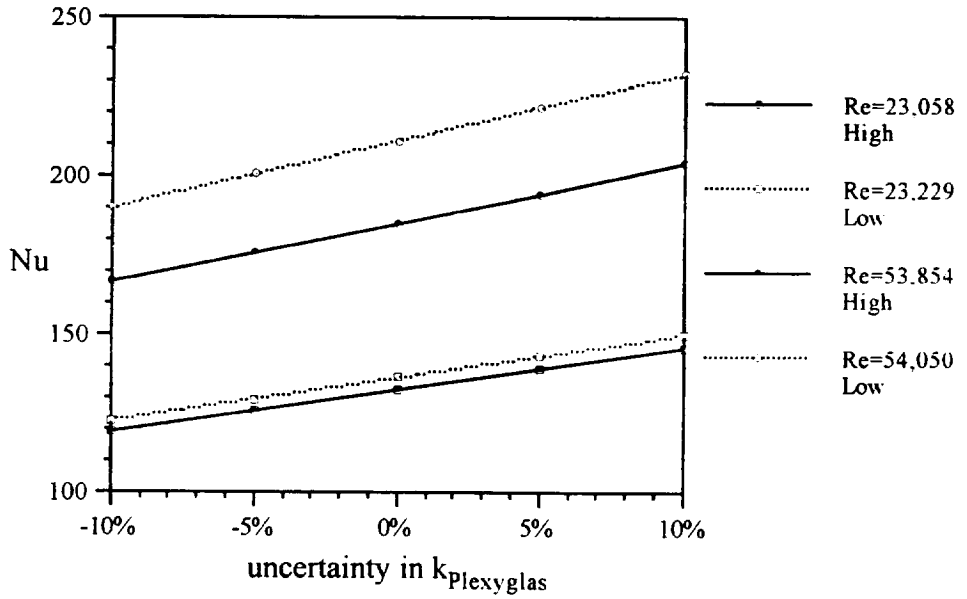

Figure 18. Stagnation Nusselt number vs. uncertainty in thermal conductivity of Plexyglas for various Reynolds numbers and heating rates.

The Nusselt number is significantly more sensitive to the uncertainty in the thermal conductivity. If it is assumed that the TLC measures the surface temperature (x=0), the analytical solution can be simplified to be a function only of the thermal product ($kc_p\rho$) as shown in Eq. 5. With this simplification, the following sensitivity graph was generated. The sensitivity of Nusselt number to the uncertainty in the thermal properties is reduced to a square root function of the uncertainty in the thermal product.

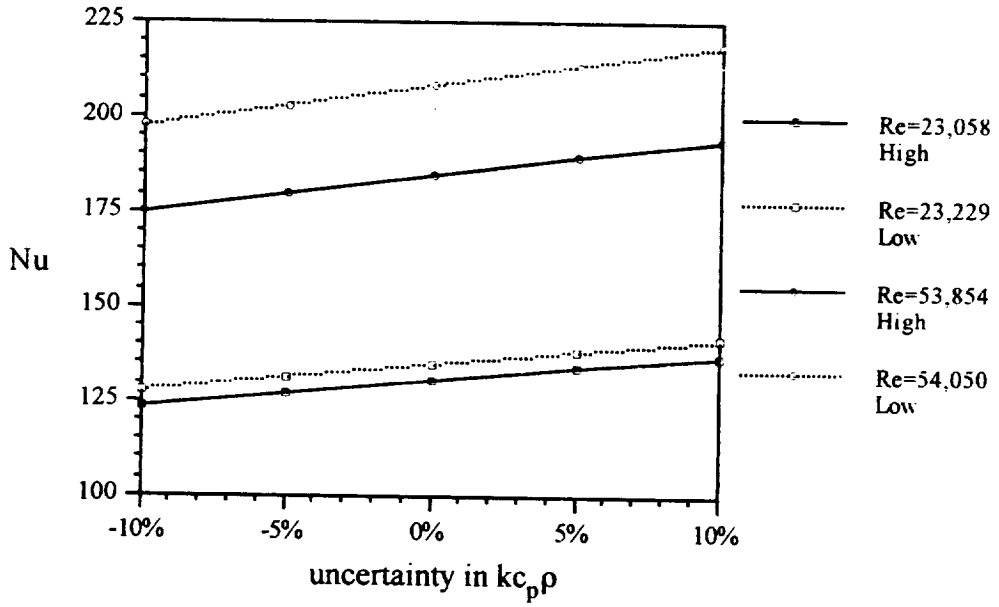

Figure 19. Stagnation Nusselt number vs. uncertainty in the thermal product of Plexyglas for various Reynolds numbers and heat rates.

Sensitivity of Nusselt number to the timing of the system

For impinging jets with very high heat transfer near the stagnation point, the transition of the TLC occurs very quickly. Therefore, the measure of time is very crucial to the evaluation of heat transfer coefficients. As mentioned earlier, the experiment was timed using the clock built into the IBM-compatible computer. A relative accuracy of ±1/36.4 of a second (27.5 milliseconds) was claimed. Assuming the uncertainty stated above as the possible error in the detection of transition time of the

TLC, the deviation in Nu corresponding to the experiment with the fastest transition time was determined, and is shown in Fig. 20.

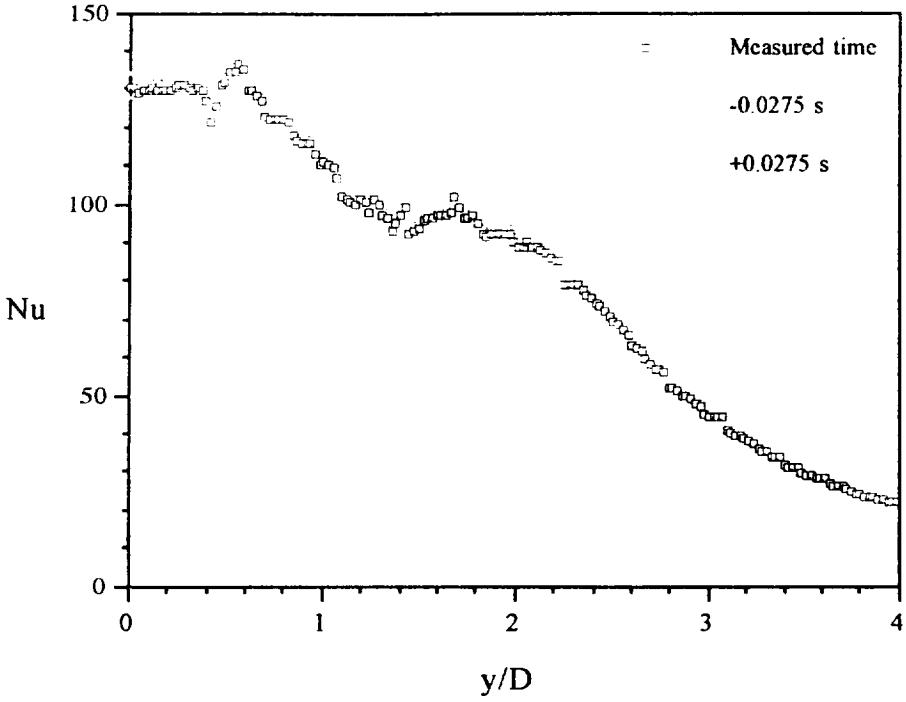

Figure 20. Sensitivity of Nu to the uncertinty in timing of the system.

The uncertainty in Nusselt number in the region near the stagnation point was about ±2%, and the uncertainty decreases significantly for locations away from the stagnation point. Also, the time required for the TLC to respond to the change in temperature has been suggested to be approximately 30 milliseconds [1]. If the Nusselt numbers are corrected for this lag time, the lower transition times will correspond to a higher Nu (approximately that of the higher curve in Fig. 20). However, the amount of correction is small, and to correct for it here without making similar adjustment for the thermal lag of other instruments, such as the thermocouples, might actually be counterproductive.

Timing using the computer is acceptable for the accuracy of the experiment, but the sequencing associated with image digitization and data acquisition must be reviewed.

Error of Nusselt number due to radiation heat loss and radial conduction

Due to thermal radiation to the ambient and radial conduction in the Plexiglas, the local heat transfer coefficient measured might be skewed. To consider the magnitude of the heat loss due to radiation, the heat flux at the surface due to the heated air is compared to that of the radiation heat flux. A conservative value of 0.9 for the emittance of the black paint was selected. The graph of the radiation heat flux and heat flux at the surface due to impinging heated jet is shown on Fig. 21. The radiation heat loss at the maximum point was only 2-3 percentage of the convection heat flux.

One-dimensionality was assumed for the temperature response of the semi-infinite slab. To validate this assumption, magnitude of the local heat flux in the axial direction is compared to the local heat flux in the radial direction. The temperature gradient in the axial direction was evaluated by taking the derivative of Eq.(4) with respect to x and evaluated at the time of TCL transition for x=0. To evaluate the temperature gradient in the radial direction, a finite difference is applied to two adjacent point on the surface for which the local heat transfer coefficients and the associated temperatures are known by applying Eq.(4). The results are shown in Fig. 21 along with heat flux from radiation and convection. For most circumstances, heat flux in the radial direction was less that 2% of the value in the axial direction. In the extreme case with high discontinuity in the measured local heat transfer coefficients, the radial heat flux reached 5% of the axial value. This high discontinuity in the local heat transfer coefficients is result of the random errors associated with the experiment, and therefore the calculated radial heat flux from a discontinious profile is not representative of the actual conduction in the plate.

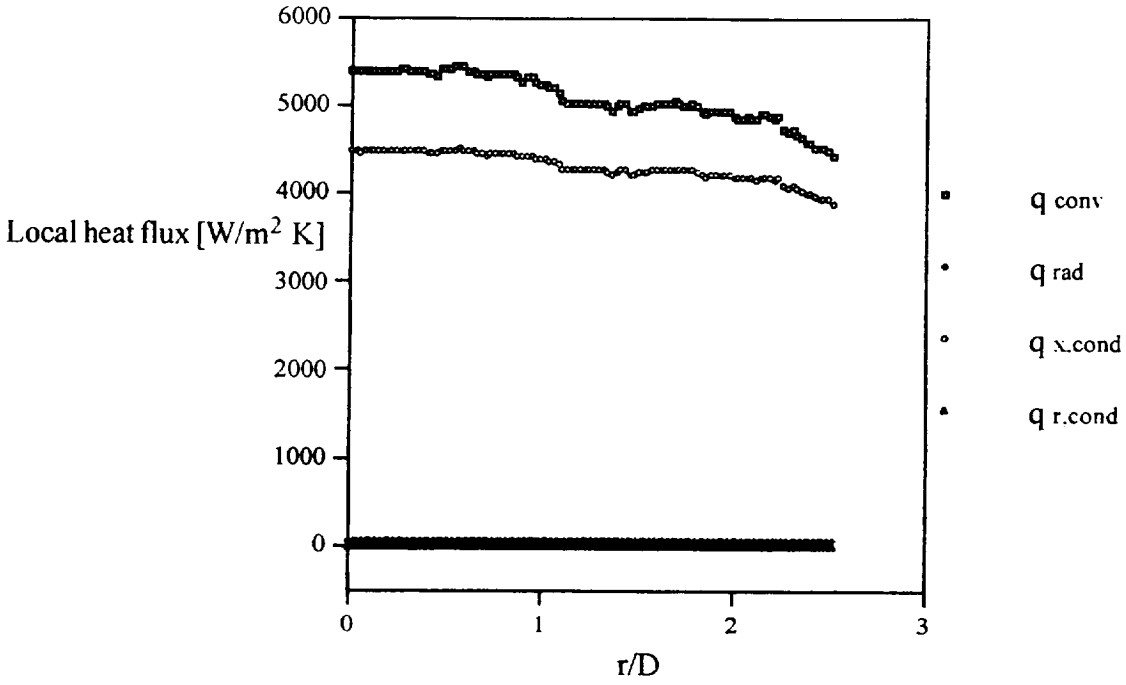

Figure 21. Comparison of local heat flux due to convection from the heated jet, radiation from the plate, axial conduction within the plate, and radial conduction within the plate at the time of TCL transition.

Summary and conclusions

A transient method with time varying free-stream temperature, using thermochromatic liquid crystal as the surface temperature indicator, was developed to determine local Nusselt numbers. By incorporating many instruments readily available for digital image capturing and data acquisition, a highly automated and easily implemented process was achieved. As with any non-conventional method, it must be validated. This was accomplished by comparing the results from this method with those from a steady-state method for a circular jet impinging onto a flat plate, and by careful error analysis of the many parameters involved.

For the first comparison, experimental data were collected for Re=23,000 and z/D=6. At this plate distance, the reduction in effectiveness in the heat jet to transfer the energy to the surface due to entrainment in ambient air was significant enough so that legitimate comparison between the two methods could not be made. Therefore, further data were collected at the same Reynolds number for a smaller plate distance of z/D=2. In addition, to provide an understanding of the effects of jet velocity, temperature of the jet at the nozzle, and other parameters on Nusselt number, two additional sets of data at Re=40,000 and 54,000 with three different heating rates for each Reynolds number were obtained.

At the same Reynolds number, the experimentally determined Nusselt numbers were consistently higher for the case of the lower heating rates. The amount of increase in the Nusselt numbers, due to the change in heating rate was more significant for the higher Reynolds numbers. The deviation in the Nusselt numbers were mostly explained when the recovery temperature of the jet was accounted for. At the highest heating rate, the difference in temperature between the jet at the nozzle and plate temperature was large enough for the increase in jet temperature due to thermal recovery

to be insignificant. In addition, at the higher Reynolds number, the higher jet velocity increased the recovery temperature of the jet. When the recovery temperature of the jet was incorporated into the analysis, the Nusselt numbers at the lower heating rates approached the Nusselt numbers at the highest rate, which remained relatively unchanged for all three sets of Reynolds number. The Nusselt numbers obtained from the current method were compared to data obtained using the steady-state method. The Nusselt numbers near the stagnation region were slightly lower than those of the steady-state method. Beyond the stagnation region, and up to 1.7 diameters downstream where the entrainment effects begin to play a role, the two methods compared very well.

To determine the recovery temperature, a crude approximation of recovery factor $r=Pr^{1/3}$ was made at all locations on the surface. It is somewhat appropriate near the stagnation region, but may be inappropriate for regions away from the stagnation point. By conducting the experiment at high difference in the jet and the plate temperature, the difficult procedure to determine the recovery factor was completely eliminated.

The sensitivity of the Nusselt number to uncertainties in various parameters was considered. First, the error in Nusselt number resulting from uncertainty in TLC transition temperature of 0.1°C was determined to be less than 6%. This error was reduced for cases where the temperature of the jet was increased significantly above the temperature of the plate. Secondly, with the application of the black background, the TLC no longer measures the surface temperature, but instead the temperature at the location of the TLC. Assuming that the TLC had similar thermal properties as the Plexiglas, the sensitivity of the Nusselt number for any given paint thickness was determined to be highest for the higher heating rates due to increased deviation of the temperature measured by the TLC at some depth to the temperature at the x=0 location.

The uncertainty in the thickness of the paint as well as lack of consistency over a given surface from the current method requires an improved method for the application of the paint. Thirdly, different lighting conditions were considered to determine any effects on the measured Nusselt number. The discrepancies in the Nusselt numbers for the many lighting variations were small with no obvious dependence. Lastly, the sensitivity of the Nusselt number to the thermal properties of the Plexiglas and the timing of the TLC transition measured by the computer was determined to be small.

Appendix A : Thermal properties of Plexiglas and air used in SLOPE

Following are the thermal properties of Plexiglas G obtained from the manufacturer [22].

Thermal Property	SI Units	British Units
Thermal conductivity	0.1875 W/(m•K)	1.3Btu/(hr)/(sq•ft)/(°F/in)
Specific heat @ 30°C (77°F)	1465.38 J/(kg•K)	0.35 BTU/(lb•°F)
Density	1190 kg/m^3	

The following three graphs are the thermal properties obtained from Table A.7 of [23].

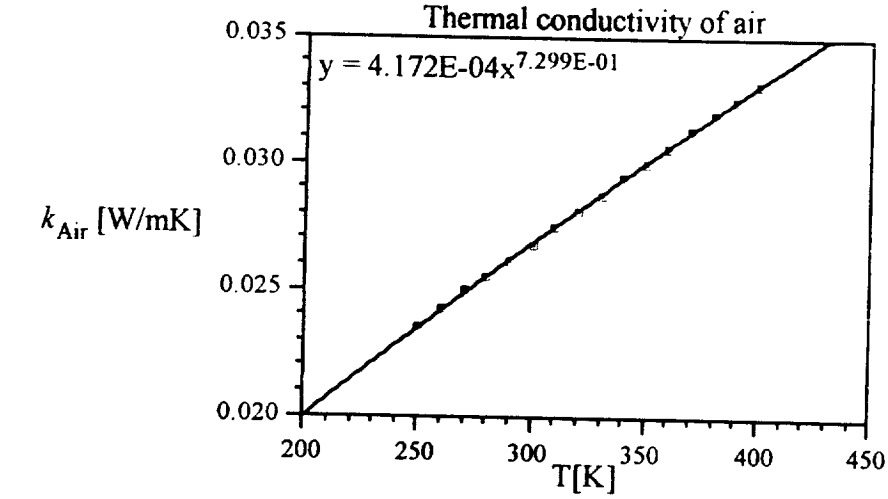

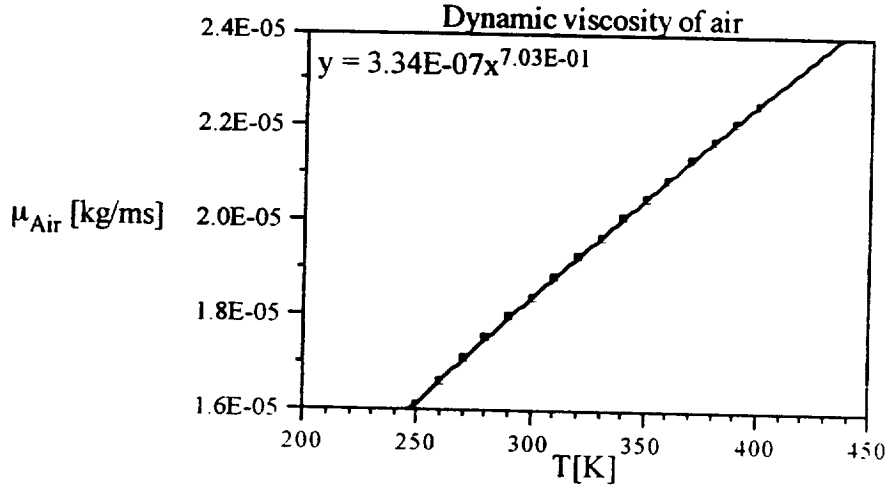

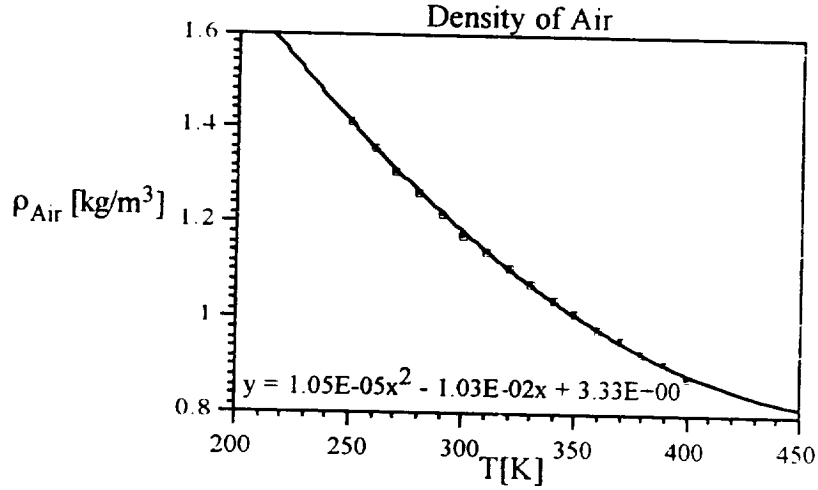

Appendix B : Equipment Summary

Encapsulated TLC

HALLCREST PRODUCTS
1820 Pickwick Lane
Glenview, Illinois 60025, U.S.A.
(708)998-8580

Model	BM/R35C1Q/C17-10
Boiling point	100°C
Melting point	0°C

Plexiglas G

8" x 9" x 1/2" (20.32 cm x 22.86 cm x 1.27 cm)
Thermal properties - See Appendix C

Nozzle

Stainless Steel pipe, 7" long
1/2" OD, 18 Gage, I.D. 10.211 mm, reamed to 11.049 mm

Data Acquisition Card

Strawberry Tree Incorporated
160 South Wolfe Road, Sunnyvale, CA 94086
(408)736-8800

MINI-16	8 16-bit Analog Input 12 Digital I/O
T21B	Terminal panel w/ reference temperature block

CCD Video camera

SONY
XC-75/75CE

Turbine Flowmeter

E G & G Flow Technology
FT-16NEXA-GEA-2
TWA-A-3

Calibration	±0.3% of reading
Repeability	±0.2% of reading
Linearity	±0.1% of reading

Pressure Transducer

Viatran Corporation
300 Industrial Dr.
Grand Island, NY 14072
(716)773-1700

2406AM2AAA20
0-100 psig

Non-linearity	0.5% of Full scale
Hysteresis	0.1% of Full scale
Repeatability	0.1% of Full scale

Pressure Regulator

Moore Products Co.
Spring House, PA 19477
Model 42HA100

Filter

Parker Hannifin Corporation
Pneumatic Division
P.O. Box 901
Richland, Michigan 49083
(616)694-9411

Thermocouples

B. J. Wolfe Enterprises
Type T (Copper-Constantan) 40 Gage wire

Range	0 to 350°C
Tolerance	±0.5°C or ±0.4% of reading

Linear Programmable Power Supply

American Reliance Inc.
LPS-305

Rating	0-165 Watts

Variac

Rating	0-140 V

Air brush

Badger

Model	200
Design pressure	15-50 psi
Recommended pressure	30 psi

Precision resistor

Vishay Resistors

Model	S102C
Value	250R
Tolerance	±0.01

References

1. Fergason, J. L., "Liquid Crystal" *Scientific American* Vol. 211, No. 2, pp. 76-86, Aug. 1964
2. Hippensteele, S. A., Russell, L. M., Stepka, F. S., "Evaluation of a Method for Heat Transfer Measurements and Thermal Visualization Using a Composite of a Heater Element and Liquid Crystals," NASA Technical Memoranda 81639
3. Korger, M., Krizek, F., "Mass-Transfer Coefficient in Impingement Flow From Slotted Nozzles" *International Journal of Heat and Mass Transfer* Vol. 9 pp.337-344
4. Gardon, R., Cobonpue, J., "Heat Transfer Between a Flat Plate and Jets of Air Impinging on It" *Proc. Second Int. Heat Transfer Conf*, pp. 454-460.
5. "Handbook of Thermochromatic Liquid Crystal Technology" HALLCREST, Liquid Crystal Division, 1820 Piccwick Lane, Glenview, Illinois 60025
6. Venneman, D., Butesfisch, K. A., "The Application of Temperature-Sensitive Crystals to Aerodynamic Investigations," European Space Agency, ESRO-RR-77, Translation of DLR-BD-73-121, 1973
7. den Ouden, C., Hoogendoorn, C. J., "Local Convective-Heat-Transfer Coefficients for Jets Impinging on a Plate; Experiments Using a Liquid Crystal Technique," Proceedings of the 5th International Heat Transfer Conference, Vol. 5, AIChE, New York, pp. 293-297, 1974
8. Cooper, T. E., Field, R. J., Meyer, J. F., "Liquid Crystal Thermography and Its Application to the Study of Convective Heat Transfer" ASME *Journal of Heat Transfer* , Vol. 97, pp. 442-450.

9. Hippensteele, S. A., Russell, L. M., Torres, F. J., "Use of a Liquid-Crystal and Heater-Elements Composite for Quantitative, High-Resolution Heat-Transfer Coefficients on a Turbine Airflow Including Turbulence and Surface-Roughness Effects," NASA Technical Memoranda 87355

10. Metzger, D. E., Larson, D. E., "Use of Melting Point Surface Coating for Local Convection Heat Transfer Measurements in Rectangular Channel Flows With 90-deg Turns", ASME *Journal of Heat Transfer* , Vol. 108, pp. 48-54, Feb., 1986

11. Saabas, H. J., Arora, S. C., Messeh, W. Abdel, "Application of the Transient Test Technique to Measure Local Heat Transfer Coefficient Associated with Augmented Airfoil Cooling Passages" Gas Turbine Conference and Exhibition Anaheim California May 31-June 4, 1987

12. Metzger, D. E., Larson, D. E., "Use of Melting Point Surface Coating for Local Convective Heat Transfer Measurments in Rectangular Channel Flows With 90° Turns" *Journal of Heat Transfer*, Vol. 108, pp48-54, Feb. 1986

13. Baughn, J. W., Ireland, P. T., Jones, T. V., Saniei, N., "A Comparison of the Transient and Heated-Coating Methods for the Measurement of Local Heat Transfer Coefficients on a Pin Fin," Journal of Heat Transfer Nov. 1989, Vol. 111, pp. 877-881

14. Akino, N., Kunugi, T., Ichimiya, K., Mitsushiro, K., Ueda, M., 1989 "Improved Liquid-Crystal Thermometry Excluding Human Color Sensation," *Journal of Heat Transfer*, Vol.111, May, pp.558-565.

15. Camci, C., Kim, K., Hippensteele, S. A., Poinsatte, P. E., 1993 "Evaluation of a Hue Capturing Based Transient Liquid Crystal Method for High Resolution Mapping of Convective Heat Transfer on Curved Surfaces," Journal of Heat Transfer, Vol. 115, pp.311-318.

16. Wang, Z., Ireland, P. T., Jones, T. V., "An Advance Method of Processing Liquid Crystal Video Signals From Transient Heat Transfer Experiments," ASME Paper 93-GT-282

17. Farina, D., J., Hacker, J., M., Moffat, R., J., Eaton, J., K., "Illuminant Invariant Calibration of Thermochromatic Liquid Crystals" *Experimental Thermal and Fluid Science* 1994; 9:1-12

18. Chan, T., L., Jambunathan, K., Leung, T., P., Ashforht-Frost, S., "A Surface Temperature Calibration Method for Thermochromatic Liquid Crystals Using True-Colour Image Processing"

19. von Wolfersdorf, J., Hoecker, R., Sattelmayer, T., "A Hybrid Transient Step-Heating Heat Transfer Measurement Technique Using Heater Foils and Liquid-Crystal Thermography" *Journal of Heat Transfer* Vol. 115 pp.319-324

20. Baughn, J. W., Shimizu, S., "Heat Transfer Measurments From a Surface With Uniform Heat Flux and an Impinging Jet" *Transaction of the ASME*, v.111, pp 1096-1098, Nov. 1989

21. Baughn, J. W., Hechanova, A. E., Yan, X., "An Experimental Study of Entrainment Effects on the Heat Transfer From a Flat Surface to a Heated Circular Impinging Jet" *Journal of Heat Transfer*, v.113, pp. 1023-1025, Nov. 1991

22. AtoHass North American, Inc., Plastic Technology Center, P.O. Box 219 Bristol, PA, 19007, Fax No. 215-781-4337, Tele No. 215-785-8290, Sandra I. Torres, AtoHaas Plastic Specialist

23. Mills, A. F, *Heat and Mass Transfer* , Irwin, Chicago 1995